



HAL
open science

Pyridinium derivatives of 3-aminobenzenesulfonamide are nanomolar-potent inhibitors of tumor-expressed carbonic anhydrase isozymes CA IX and CA XII

Suleyman Akocak, Özlen Güzel-Akdemir, Rajesh Kishore Kumar Sanku, Samson S. Russom, Bogdan Iorga, Claudiu T. Supuran, Marc A. Ilies

► To cite this version:

Suleyman Akocak, Özlen Güzel-Akdemir, Rajesh Kishore Kumar Sanku, Samson S. Russom, Bogdan Iorga, et al.. Pyridinium derivatives of 3-aminobenzenesulfonamide are nanomolar-potent inhibitors of tumor-expressed carbonic anhydrase isozymes CA IX and CA XII. *Bioorganic Chemistry*, 2020, 103, pp.104204. 10.1016/j.bioorg.2020.104204 . hal-02998386

HAL Id: hal-02998386

<https://hal.science/hal-02998386v1>

Submitted on 5 Dec 2020

HAL is a multi-disciplinary open access archive for the deposit and dissemination of scientific research documents, whether they are published or not. The documents may come from teaching and research institutions in France or abroad, or from public or private research centers.

L'archive ouverte pluridisciplinaire **HAL**, est destinée au dépôt et à la diffusion de documents scientifiques de niveau recherche, publiés ou non, émanant des établissements d'enseignement et de recherche français ou étrangers, des laboratoires publics ou privés.

Pyridinium Derivatives of 3-Aminobenzenesulfonamide are Nanomolar-potent Inhibitors of Tumor-expressed Carbonic Anhydrase Isozymes CA IX and CA XII

Suleyman Akocak,^a Özlen Güzel-Akdemir,^{b,c} Rajesh Kishore Kumar Sanku,^a Samson S. Russom^a, Bogdan I. Iorga,^d Claudiu T. Supuran,^{b*} and Marc A. Ilies^{a*}

^a Department of Pharmaceutical Sciences and Moulder Center for Drug Discovery Research, Temple University School of Pharmacy, 3307 N Broad Street, Philadelphia, PA-19140.

^b NEUROFARBA Department, Università degli Studi di Firenze, Polo Scientifico, Via della Lastruccia 3, 50019 Sesto Fiorentino (Florence), Italy.

^c Istanbul University, Faculty of Pharmacy, Department of Pharmaceutical Chemistry, 34116 Beyazıt, Istanbul, Turkey.

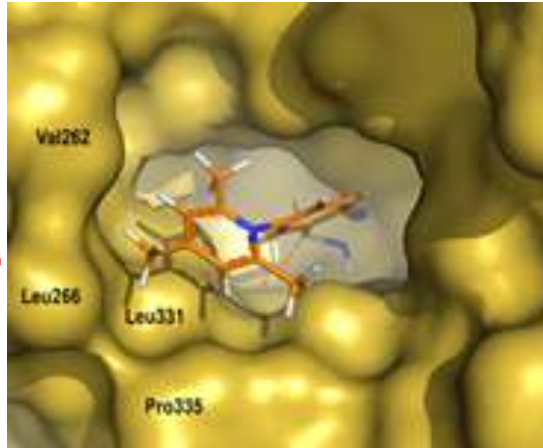
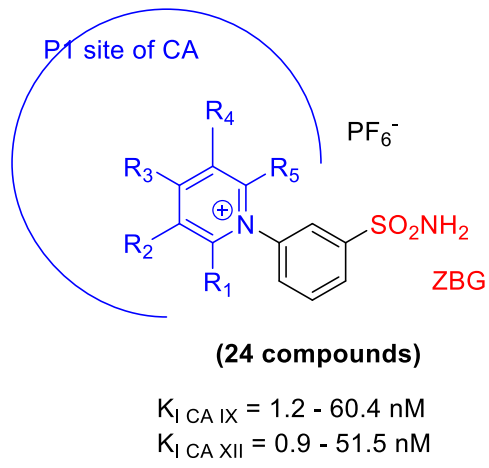
^d Université Paris-Saclay, CNRS, Institut de Chimie des Substances Naturelles (ICSN), 1 Avenue de la Terrasse, 91198 Gif-sur-Yvette, France.

*Correspondence authors: CTS: Phone: +39-055-4573005; Fax: +39-055-4573385; E-mail: claudiu.supuran@unifi.it; MAI: Phone: 215-707-1749; Fax 215-707-5620; Email: mailies@temple.edu;

Abstract: Building on the conclusions of previous inhibition studies with pyridinium-benzenesulfonamides from our team and on the X-ray crystal structure of the lead compound identified, a series of 24 pyridinium derivatives of 3-aminobenzenesulfonamide was synthesized and investigated for carbonic anhydrase inhibition. The new pyridinium-sulfonamides were evaluated as inhibitors of four human carbonic anhydrase (CA, EC 4.2.1.1) isoforms, namely CA I, CA II (cytosolic), CA IX and XII (transmembrane, tumor-associated forms). Excellent inhibitory activity in the nanomolar range was observed against CA IX with most of these sulfonamides, and against CA XII (nanomolar/sub-nanomolar) with some of the new compounds. These sulfonamides were generally potent inhibitors of CA II and CA I too. Docking studies revealed a preference of these compounds to bind the P1 hydrophobic site of CAs, supporting the observed inhibition profile. The salt-like nature of these positively charged sulfonamides can further focus the inhibitory ability on membrane-bound CA IX and CA XII and could efficiently decrease the viability of three human carcinomas under hypoxic conditions where these isozymes are over-expressed, thus recommending the new compounds as potential diagnostic tools or therapeutic agents.

Keywords: carbonic anhydrase, isozyme, inhibitor, pyridinium, sulfonamide, tumor growth

Graphical Abstract:



Introduction

The tremendous advances in medicine achieved in the last century increased human life expectancy significantly. As a consequence of increased lifespan, various genetic and epigenetic mutations in the human genome that result in the loss of function of tumor suppressor genes and/or gain of function or hyperactivation of oncogenes became more and more prevalent, yielding different forms of cancers. Cancer is currently the second most common cause of death and a major cause of mortality in the world. Multiple mutations and epigenetic changes are believed to confer a selective advantage towards tumor cell proliferation and survival [1]. As the tumor tissue grows fast, subpopulations of tumor cells encounter different constraints such as lack of oxygen (hypoxia) and nutrients caused by abnormal tumor vasculature [2]. This deficient environment forces the tumor cells to initiate response mechanisms that favor cell survival and migration. In this context, it must be emphasized that a general hallmark of over 70% of solid tumors is their hypoxic nature [2]. Malignant cells uncontrolled growth consumes nutrients and oxygen at a pace that cannot be sustained by the existent local vasculature. Hypoxia stabilizes the cytosolic HIF-1 α , which accumulates in the cytoplasm under hypoxic conditions and subsequently translocates to the nucleus, where it forms a heterodimer with the constitutively stable HIF-1 β subunit. Subsequently, the activated HIF complex promotes the expression of genes containing a hypoxia-responsive element (HRE) [2-4].

The hypoxic state has been strongly associated with malignant progression and resistance to chemo- and radiotherapy in many tumor types [5, 6]. An examination of tumor biochemistry reveals that hypoxic tumors rely on glycolysis as main energy source. The inefficiency of glycolysis towards ATP production determines a dramatic increase in the glucose consumption in hypoxic tumors. Thus, among the genes upregulated by HIF-1 are genes encoding key proteins

involved in angiogenesis (e.g. vascular endothelial growth factor, VEGF), glucose transport (GLUT), glycolysis (e.g. phosphofructokinase 1, PFK-1), export of monocarboxylic acids (e.g. monocarboxylate transporter, MCT), and the gene encoding a membrane-bound isozymes of carbonic anhydrase, namely CA IX and CA XII (Figure 1) [7-10], which are strongly expressed under hypoxic conditions [11]. Thus, carbonic anhydrase IX (CA IX) was recognized as an endogenous marker of tumor hypoxia and its elevated expression has been independently associated with poor prognosis in a large number of tumor types [12-17]. Interestingly, CA IX is the most strongly overexpressed gene in response to hypoxia in human cancer cells [18-20]. Normal tissue expression of CA IX is restricted to epithelia of the stomach, small intestine and gall bladder [9, 17, 21]. A similar over-expression profile in tumor cells was shown to be valid for CA XII, another plasma membrane-associated isozyme [7, 20, 22-25]. It was shown that both CA IX and CA XII have a critical role in maintaining intracellular pH within normal levels in the highly metabolically active cancer cells and were also proved to be critical for tumor cell growth and survival (Figure 1) [7, 20, 26-31].

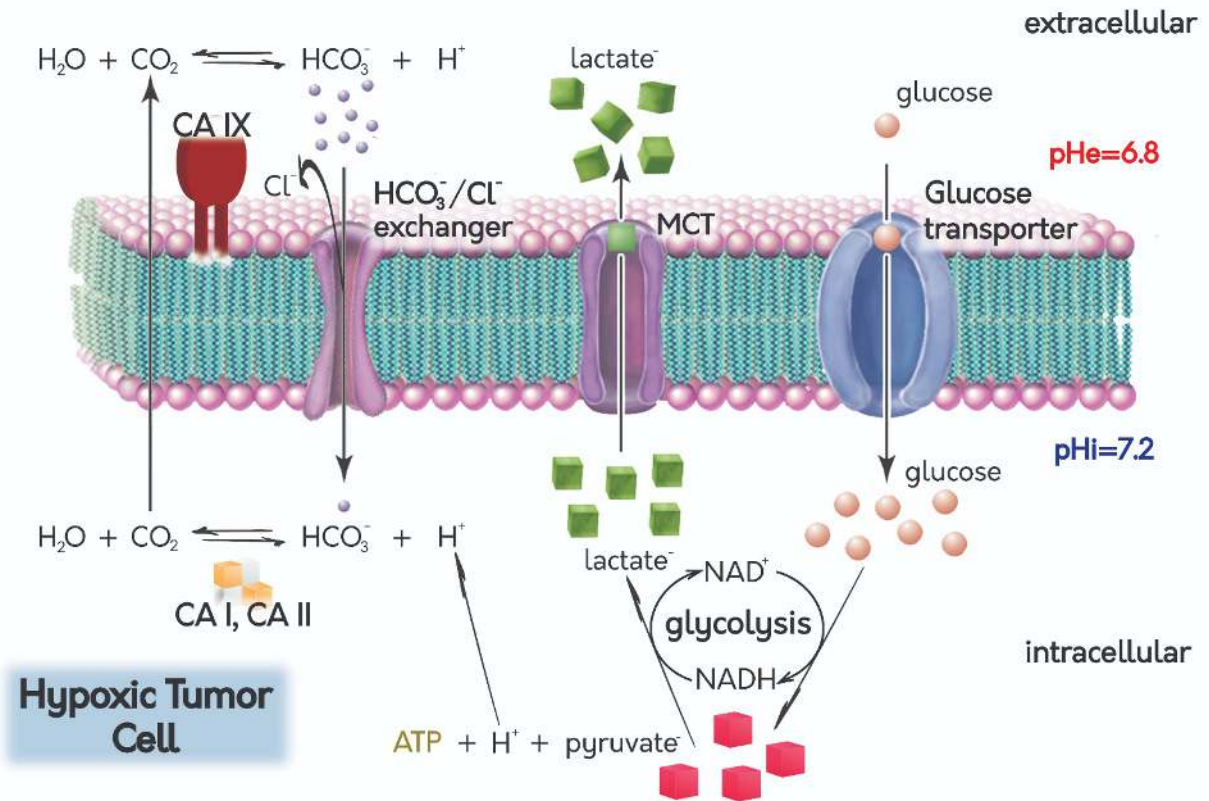


Figure 1. Schematic depiction of acidosis in hypoxic tumors as a result hypoxia, emphasizing the upregulation of glycolysis and the central role played by carbonic anhydrases in maintaining the intracellular pH and acidification of external tumor milieu.

Thus, carbonic anhydrases (CAs, E. C. 4.2.1.1) are a class of ubiquitous metalloenzymes evolved to efficiently catalyze the reversible hydration of carbon dioxide $CO_2 + H_2O \rightleftharpoons HCO_3^- + H^+$. They are found in virtually all living organisms, from the unicellular ones to higher vertebrates. Their structure is encoded by eight evolutionary unrelated gene families, namely, α -, β -, γ -, δ -, ζ -, η -, θ -, and ι -CAs. [7, 32-35] Fourteen CA isozymes (hCAs), all belonging to the α -class, are currently known in humans, with different tissue and organ distribution, subcellular localization and catalytic properties. One can distinguish cytosolic isozymes (CA I, CA II, CA III,

CA VII, and CA XIII), membrane-bound isoforms (CA IV, CA IX, CA XII, and CA XIV), mitochondrial isozymes (CA VA and CA VB) and even secreted isozymes (CA VI). [7, 32, 33, 36].

The above-mentioned carbonic anhydrase isoforms are involved in critical physiologic and pathologic processes in the human body, which include respiration and transport of CO₂ from tissues to lungs, acid-base regulation and pH homeostasis, electrolyte secretion in various tissues and organs, bone resorption/calcification, biosynthetic reactions such gluconeogenesis, lipogenesis and ureagenesis, tumorigenicity, etc. Some of these isoforms are over-expressed in pathological conditions such as edemas, glaucoma, obesity and cancer, making them important targets for pharmaceutical research [40, 51, 52, 54, 62, 63]. As mentioned above, CA IX and CA XII are over-expressed in many tumors where they are involved in pH regulation, cell adhesion and tumor progression. Therefore, targeting of CA IX and CA XII isozymes with selective inhibitors, antibodies and (radio)immunoconjugates constitutes a promising approach to anticancer therapy in general [7, 20, 32, 37-49].

Among these various classes of CA inhibitors (CAIs), aromatic and heterocyclic primary sulfonamides are the most investigated and used CAIs in physiological and pharmacological studies, as well as in clinical use. Rigorous selection of the most efficient aromatic and heterocyclic systems and further optimizations of the pendant moieties yielded the clinically used inhibitors acetazolamide **1**, methazolamide **2**, ethoxzolamide **3**, benzolamide **4**, dichlorphenamide **5** (Chart 1) [7, 32, 38, 41-46, 48, 50]

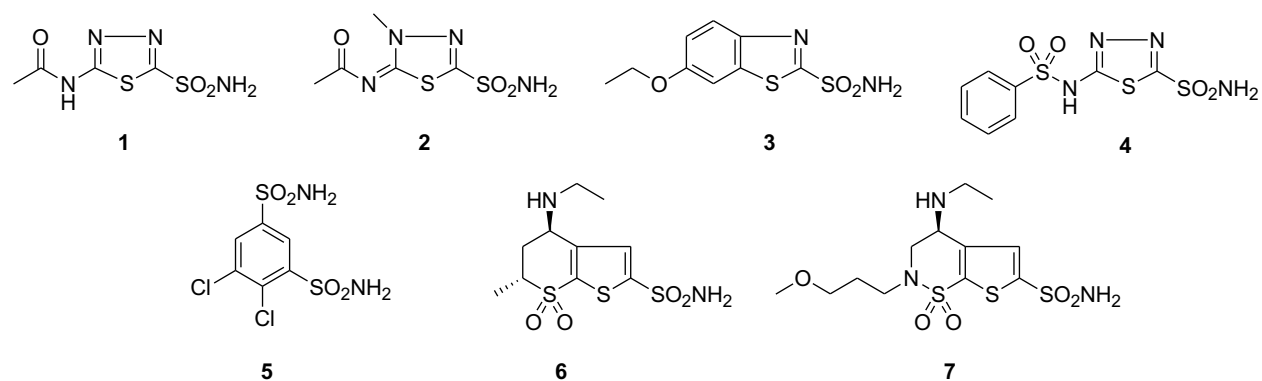


Chart 1. CA inhibitors in clinical use, designed either for systemic use (**1-5**) or for topical administration into the eye (**6 and 7**).

However, it was established that clinically used CA inhibitors (CAIs) **1-5**, initially designed for efficient inhibition of CA II, are quite potent against the other CA isozymes [7, 32, 34, 38, 41-46, 48]. The low isozyme selectivity of these sulfonamides can be explained by the relatively high sequence homology of CA isoforms. Since these drugs have a good tissue penetrability, their systemic use is associated with serious side effects such as fatigue, metallic taste, decreased libido, paresthesia, etc. due to inhibition of all CA isozymes in the human body [7, 32, 38, 41-46, 48]. One way to reduce the extent of the side-effects associated with their use is through topical administration of the CAI. Dorzolamide **6** and brinzolamide **7** were developed for the treatment of glaucoma via topical administration into the eye [7, 32-34, 41, 43, 51]. Another way to increase isozyme selectivity is to exploit the structural differences that exist between the active site of various CA isozymes by conjugating the classical aromatic/heterocyclic warheads with moieties of different sizes and lipophilicities (the “tail approach”) [7, 32-34, 41, 43, 51, 52]. This strategy was used to find potent and selective inhibitors for CA IX in the first inhibition study of this isozyme with sulfonamides [40]. In this study, two CAI scaffolds sulfanilamide and aminobenzolamide were derivatized with different halogens of increased steric bulk (F, Cl, Br, I)

at selected positions of their phenyl rings for efficient sampling the active site of different CA isozymes. The most potent and selective CA IX inhibitor was 3-fluoro-5-chloro-4-aminobenzenesulfonamide **8** ($K_{I\text{hCA I}} = 3800\text{ nM}$, $K_{I\text{hCA II}} = 32\text{ nM}$, $K_{I\text{hCA IX}} = 12\text{ nM}$). Dihalogenophenyl derivatives such as **9** ($K_{I\text{hCA I}} = 1.4\text{ nM}$, $K_{I\text{hCA II}} = 0.3\text{ nM}$, $K_{I\text{hCA IX}} = 38\text{ nM}$) and congeners displayed a rather strong and uniform potency against all four isozymes, revealing the importance of the scaffold used and of the placement of the pendant groups on the main scaffold for inducing potency and selectivity against different CA isozymes, including CA IX and XII [40]. These ability to generate potent CA IX and CA XII inhibitors via tail approach was confirmed in following studies using bulky and lipophilic adamantane groups, such as **10** ($K_{I\text{hCA I}} = 883\text{ nM}$, $K_{I\text{hCA II}} = 11\text{ nM}$, $K_{I\text{hCA IX}} = 6.4\text{ nM}$, $K_{I\text{hCA XII}} = 2.8\text{ nM}$), superior homolog **11** ($K_{I\text{hCA I}} = 362\text{ nM}$, $K_{I\text{hCA II}} = 8.9\text{ nM}$, $K_{I\text{hCA IX}} = 49.5\text{ nM}$, $K_{I\text{hCA XII}} = 4.7\text{ nM}$) [53, 54] (Chart 2) and related lipophilic compounds [7, 32-34, 41, 43, 51, 55]

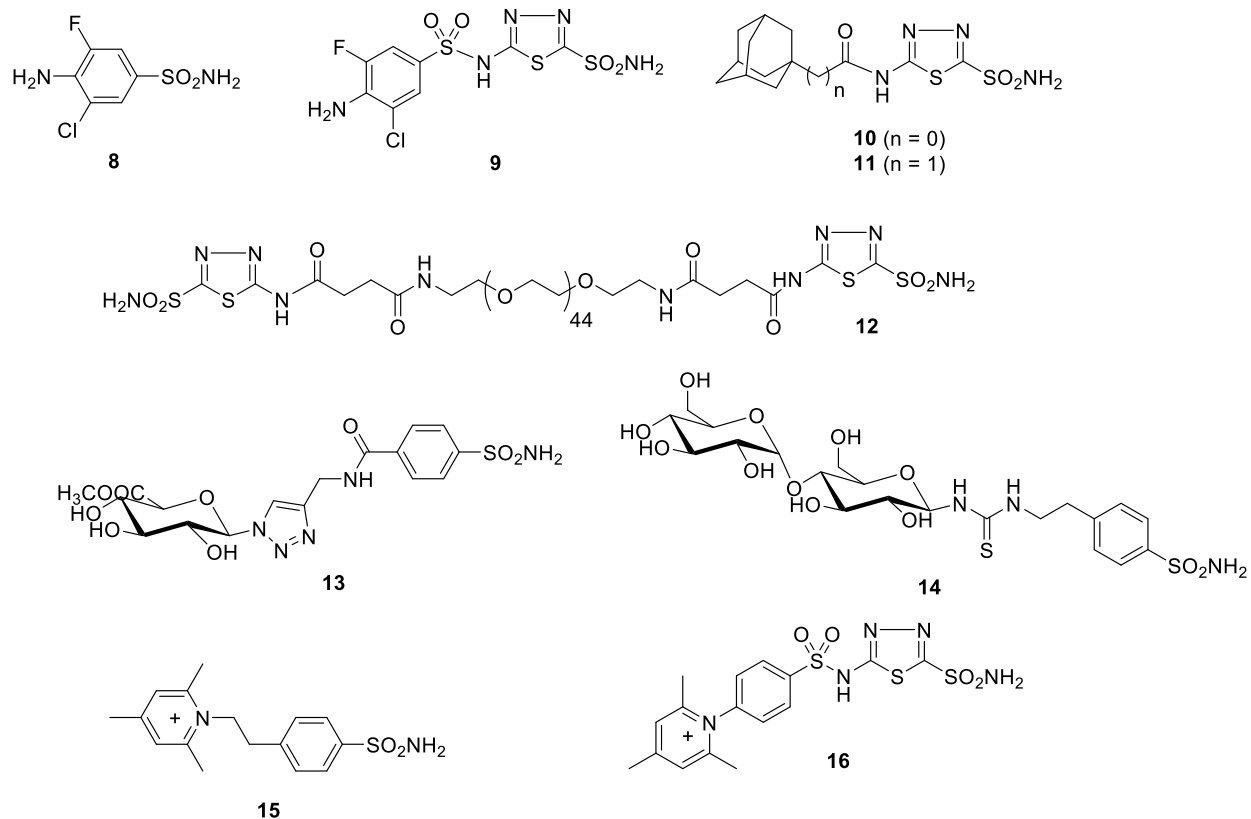


Chart 2. Lead CA inhibitors potent against CA IX and CA XII identified in previous studies

The explanation for this particular inhibition profile was provided by via X-ray crystallography of the adduct of **9** with CA II [56], and of **10** with CA II [54], which revealed that the lipophilic “tail” of the inhibitor can be accommodated either in a hydrophobic pocket delimited by amino acids Phe131, Val135, Leu198 and Pro202 (denominated P1) or in an amphiphilic pocket delimited by amino acids Phe131, Ile91 and Gln92 (denominated P2) [54, 56, 57].

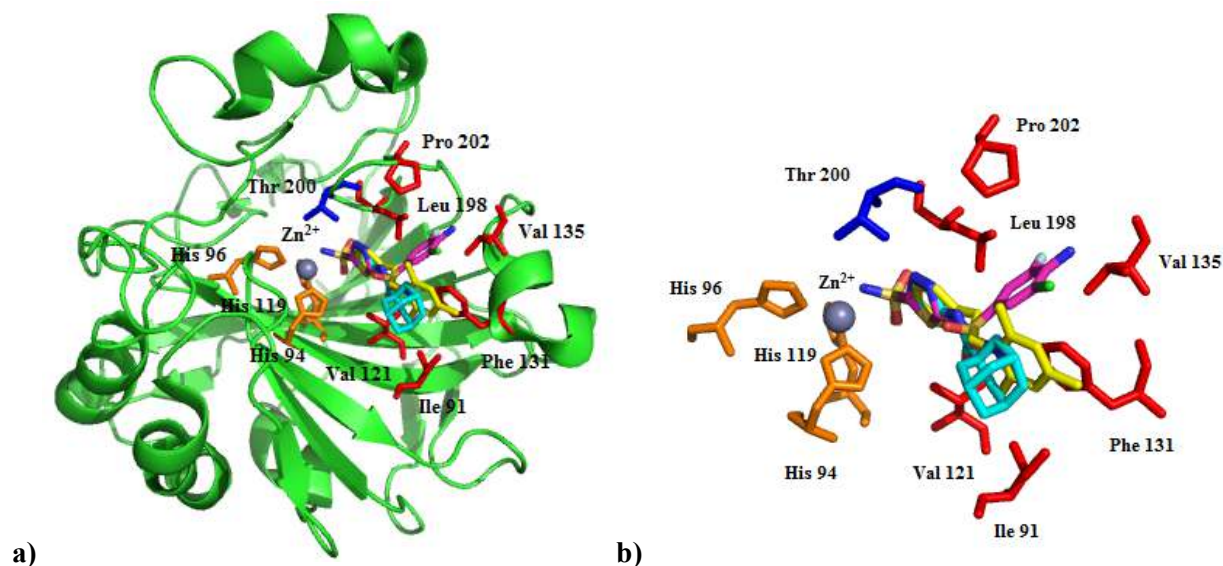


Figure 2. Ribbon diagram (a) and active site detail (b) of the hCA II in complex with inhibitors **9** (magenta, PDB code 2hoc [56]), **10** (light blue, pdb code 3mhc [54]) and **15** (yellow, PDB code 1ze8 [58]), revealing the interaction of the tail of the inhibitor with two hydrophobic/amphiphilic pockets P1 (Phe131, Val135, Leu198, Pro202) and P2 (Phe131, Ile91, Val121). Pyridinium ring of CAI **15**, located in amphiphilic pocket P2, π - π stacks with Phe131. Figure made using PyMol (DeLano Scientific).

Another frequently used strategy to achieve isozyme selectivity is through membrane-impermeant inhibitors that inhibit only the membrane-bound isozymes, leaving the cytosolic isozymes unaffected. [7, 32, 34, 38, 41-46, 48] One strategy to obtain membrane-impermeant inhibitors was through conjugation of CAI warheads with very hydrophilic moieties, either polymers such as dextran, aminoethyl dextran, polyethylene glycol [45, 59, 60], such as **12** ($K_{I_{hCA I}} = 225$ nM, $K_{I_{hCA II}} = 66$ nM, $K_{I_{hCA IX}} = 2.5$ nM, $K_{I_{hCA XII}} = 5.4$ nM), [45] or with sugar moieties [61-66], such as **13** ($K_{I_{hCA I}} = 2.4$ nM, $K_{I_{hCA II}} = 378$ nM, $K_{I_{hCA IX}} = 23$ nM) [62] and **14** ($K_{I_{hCA I}} = 4260$ nM, $K_{I_{hCA II}} = 271$ nM, $K_{I_{hCA IX}} = 2.1$ nM, $K_{I_{hCA XII}} = 9.8$ nM) [65] (Chart 2). Another strategy for the generation of membrane-impermeant sulfonamide inhibitors is through

conjugation of aromatic and heterocyclic sulfonamide warheads with permanently charged groups. Our team proposed the conjugation of aromatic and heterocyclic amino-sulfonamides with pyridinium positively charged moieties, generated via reaction of pyrylium salts with primary amino groups [67-71]. Efficient sampling of the active site of CA isozymes was achieved through the use of substituents with different shapes and steric demands on pyridinium ring, generating nanomolar potent positively charged sulfonamides such as **15** ($K_{I\text{hCA I}} = 4 \mu\text{M}$, $K_{I\text{hCA II}} = 21 \text{ nM}$, $K_{I\text{hCA IX}} = 14 \text{ nM}$, $K_{I\text{hCA XII}} = 7 \text{ nM}$), [7, 69, 72] or **16** ($K_{I\text{hCA I}} = 18 \text{ nM}$, $K_{I\text{hCA II}} = 4 \text{ nM}$, $K_{I\text{hCA IX}} = 5.8 \text{ nM}$, $K_{I\text{hCA XII}} = 48 \text{ nM}$) [68, 73] (Chart 2). The salt-like nature of these pyridinium sulfonamides does not allow them to cross biological membranes, inhibiting the membrane-bound isozymes while leaving unaffected the cytosolic CA I and CA II, as proved by in vitro and in vivo studies [7, 69, 74].

An examination of the binding mode of pyridinium sulfonamide **15** in the active site of CA II revealed that the pyridinium ring extends in the P2 site of the enzyme, delimited (in CA II) by residues Phe131, Ile91 and Val121 and π - π stacks with Phe-131 residue of the CA II active site (Figure 2) [58]. The sampling of this pocket is possible because the pyridinium moiety is attached to the phenyl ring in the para position related to sulfonamide group via a flexible ethyl linker as in compound **15**. One can hypothesize that if the pyridinium ring would be attached directly to the phenyl moiety of the inhibitor in the meta position it could access directly both P1 and P2 pockets. Importantly, CA IX and CA XII have a much larger P1 and P2 sites than CA II (Phe131 is replaced by a Val in CA IX and by an Ala in CA XII) and other amino acids flanking these two pockets are different in these CA isozymes (e.g. residues 91, 135, 204). Since the size, shape and lipophilicity of these two pockets depend directly on these key amino acid residues, it can be expected that substitution of pyridinium ring with lipophilic substituents of different sizes will modulate potency

and selectivity of the CAI, similarly to other studies involving CA activators [75-77]. We have decided to evaluate this hypothesis in this study, through the synthesis of novel pyridinium salts derived from 3-aminobenzenesulfonamide and through of their inhibition potency and selectivity against tumor over-expressed isozymes CA IX and CA XII and against their cytosolic counterparts CA I and CA II.

Materials and methods

Materials: 3-Aminobenzenesulfonamide, acetazolamide, triethylamine, acetic acid, acetic anhydride were from Sigma Aldrich (St Louis, MO), Alfa Aesar/VWR International (West Chester, PA), Across/Fisher Scientific (Pittsburg, PA) or TCI America (Portland, OR) and were used without further purification. Solvents (methanol, ethanol, dichloromethane, acetone, acetonitrile, all HPLC quality), 25% aqueous NH₄OH, 37% aqueous HCl, NaHCO₃, NaOH were purchased from EMD (Gibbstown, NJ), Fisher Scientific or VWR International and were used as received. Deionized water produced from a Millipore MilliQ system was used in all experiments that required it. Pyrylium salts were prepared as described elsewhere by monoacylation of mesityl oxide or diacylation of olefins [78].

Techniques: Reactions were monitored using thin-layer chromatography (TLC) on Sigma-Aldrich SiO₂-precoated aluminum TLC plates (silica gel with F254 indicator, pore size 60 Å, layer thickness 0.20 mm), eluted with MeOH:DCM, 20:80 or 10:90 (v/v).

Normal phase preparative chromatography was carried out using prepacked RediSep silica gel columns on a Combiflash Rf LC system (Teledyne Isco, Lincoln, NE). The purity of compounds was assessed via LC-MS using Agilent 1200 HPLC-DAD-MS system equipped with

a G131A DAD and a 6130 Quadrupole MS via a ZORBAX SB-C18 column, eluted with H₂O (0.1 % HCOOH)/ MeCN (0.1 % HCOOH) 95/5 to 0/100 linear gradient.

The melting points were determined via Thermolyne heating stage microscope (Dubuque, IA), equipped with an Olympus 5X objective, at heating/cooling rate of ~ 4 °C/min and were uncorrected.

The NMR spectra were recorded at 300 K, in deuterated dimethyl sulfoxide (DMSO-d₆), on a Bruker Avance III 400 Plus spectrometer equipped with a 5 mm indirect detection probe, operating at 400 MHz for ¹H-NMR, at 100 MHz for ¹³C-NMR, and at 376 MHz for ¹⁹F-NMR. Chemical shifts are reported as δ values, using TMS as internal standard for proton spectra and the solvent resonance for carbon spectra, in parts per million (ppm), and the coupling constants (J) are expressed in hertz (Hz). Peak shapes were denoted as follows: s, singlet; d, double; t, triplet; q, quadruplet; m, multiplet; bs, broad singlet. Assignments were done by means of chemical shifts, peak integration, COSY, HMQC, HMBC experiments, and model spectra.

Elemental analyses were performed by combustion, using a Perkin Elmer 2400 Series II CHNS analyzer.

General procedure for the synthesis of pyridinium 3-aminobenzene sulfonamide series 29

In a typical experiment, 3-aminobenzene sulfonamide (0.34 g, 2 mmol, 1 equiv) was dissolved in a minimum amount of EtOH (~ 5 mL) and 0.7 mL (5 mmol) of NEt₃ was added dropwise, under stirring. The reaction became homogenous in about 5 min. Separately, the pyrylium salt (1.1 equiv) was dissolved in a minimum amount of DCM or DCM/EtOH 2/1, v/v

(~5 mL), 0.25 mL (5 mmol) of Ac₂O was added and the homogenous mixture was added quickly to the 3-aminobenzene sulfonamide solution. The colored solution obtained was refluxed for 15 min, treated with 0.3 mL (5 mmol) AcOH and refluxed overnight. The next day, the reaction mixture was cooled, 0.5 mL of 25 % aqueous NH₄OH was added and the mixture was refluxed for 5 min in order to convert unreacted pyrylium salt into the corresponding pyridine. The solution was evaporated to dryness and the residue was washed with 3 x 25 mL ethyl ether. After drying under vacuum, the crude product was treated with 5 mL of 5 % aqueous HPF₆, filtered, and subsequently adsorbed on 3 g of SiO₂ using MeOH. Flash chromatography on SiO₂ using MeOH/DCM gradients afforded the pure compound, which was crystallized from EtOH/ethyl ether.

2,4,6-Trimethyl-1-(3-sulfamoylphenyl)pyridinium hexafluorophosphate (19a): mp 196-198 °C ; Yield 30.6 %; ¹H-NMR (DMSO-d⁶), δ, ppm: 7.85-8.15 (m, 4H, H-2,4,5,6 1-Ph), 7.97 (s, 2H, H-3,5 Py⁺), 7.54 (br. s, 2H, SO₂NH₂), 2.62 (s, 3H, H 4-CH₃), 2.32 (s, 6H, H- 2,6-CH₃); ¹³C-NMR (DMSO-d⁶), δ, ppm: 159.4 (C₄ Py⁺), 154.6 (C_{2,6} Py⁺), 146.3 (C₁ 1-Ph), 138.3 (C₃ 1-Ph), 131.9 (C₆ 1-Ph), 129.6 (C_{3,5} Py⁺), 128.2 (C₄ 1-Ph), 127.2 (C₅ 1-Ph), 123.5 (C₂ 1-Ph), 21.6 (C₄ Me), 21.3 (C_{2,6} Me); ¹⁹F-NMR (DMSO-d⁶), δ, ppm: -70.12 (d, J = 712 Hz, PF₆⁻); LC-MS: (C₁₄H₁₇N₂O₂S), exact mass: 277.1; Found: 277.0 (> 97%); Anal (C₁₄H₁₇N₂O₂S⁺ PF₆⁻) requires (%): C 39.82, H 4.06, N 6.63; Found: C 40.01, H 4.19, N 6.70.

2,6-Diethyl-4-methyl-1-(3-sulfamoylphenyl)pyridinium hexafluorophosphate (19b): mp 160-162 °C; Yield 45.3 %; ¹H-NMR (DMSO-d⁶), δ, ppm: 8.17 (s, 2H, H-3,5 Py⁺), 8.16 (t, H, H-5 1-

Ph), 7.90-7.99 (m, 3H, H-2,4,6 1-Ph), 7.64 (br. s, 2H, SO₂NH₂), 2.53 (s, 3H, H 4-CH₃), 2.50 (m, 4H, H 2,6-CH₂CH₃), 1.60 (s, 6H, H 2,6-CH₂CH₃); ¹³C-NMR (DMSO-d⁶), δ, ppm: 159.9 (C₄ Py⁺), 158.8 (C_{2,6} Py⁺), 146.1 (C₁ 1-Ph), 137.3 (C₃ 1-Ph), 131.6 (C₆ 1-Ph), 130.0 (C_{3,5} Py⁺), 128.3 (C₄ 1-Ph), 125.2 (C₅ 1-Ph), 123.9 (C₂ 1-Ph), 27.2 (C₁ Et), 21.5 (C₄ Me), 12.1 (C₂ Et); ¹⁹F-NMR (DMSO-d⁶), δ, ppm: -70.16 (d, *J* = 712 Hz, PF₆⁻); LC-MS: (C₁₆H₂₁N₂O₂S), exact mass: 305.1; Found: 305.0 (> 97%); Anal (C₁₆H₂₁N₂O₂S⁺ PF₆⁻) requires (%): C 42.67, H 4.70, N 6.22; Found: C 42.76, H 4.78, N 6.31.

4-Methyl-2,6-di-n-propyl-1-(3-sulfamoylphenyl)pyridinium hexafluorophosphate (19c): mp 206-209 °C; Yield 20.6 %; ¹H-NMR (DMSO-d⁶), δ, ppm: 8.16 (s, 2H, H-3,5 Py⁺), 7.90-8.15(m, 4H, H-2,4,5,6 1-Ph), 7.67 (br. s, 2H, SO₂NH₂), 2.65 (s, 3H, H 4-CH₃), 2.45 (m, 4H, H 2,6-CH₂CH₂CH₃), 1.28 (m, 4H, H 2,6-CH₂CH₂CH₃), 0.79 (t, 6H, H 2,6- CH₂CH₂CH₃); ¹³C-NMR (DMSO-d⁶), δ, ppm: 159.9 (C₄ Py⁺), 158.8 (C_{2,6} Py⁺), 146.1 (C₁ 1-Ph), 137.3 (C₃ 1-Ph), 131.6 (C₆ 1-Ph), 130.0 (C_{3,5} Py⁺), 128.3 (C₄ 1-Ph), 125.2 (C₅ 1-Ph), 123.9 (C₂ 1-Ph), 27.2 (C₁ n-Pr), 21.5 (C₄ Me), 12.1 (C₂ n-Pr); ¹⁹F-NMR (DMSO-d⁶), δ, ppm: -70.15 (d, *J* = 712 Hz, PF₆⁻); LC-MS: (C₁₈H₂₅N₂O₂S), exact mass: 333.2; Found: 333.1 (> 97%); Anal (C₁₈H₂₅N₂O₂S⁺ PF₆⁻) requires (%): C 45.19, H 5.27, N 5.86; Found: C 45.22, H 5.34, N 5.89.

2,6-Diisopropyl-4-methyl-1-(3-sulfamoylphenyl)pyridinium hexafluorophosphate (19d): mp 150-155 °C ; Yield 34 %; ¹H-NMR (DMSO-d⁶), δ, ppm: 8.26-8.20 (br. s, 2H, H-3,5 Py⁺), 8.17 (dt, *J* = 1.4, 7.8 Hz, 1H, H-2 1-Ph), 8.03 (dt, *J* = 1.4, 7.8 Hz, 1H, H-6 1-Ph), 7.97 (t, *J* = 7.8 Hz, 1H, H-4 1-Ph), 7.69 (br.s, 2H, SO₂NH₂), 3.79 (hep, *J* = 6.1 Hz, 2H, H 2,6-CH(CH₃)₂), 2.69 (s, 3H,

H 4-CH₃), 1.22 (d, *J* = 6.7 Hz, 3H, CH₃A from 2-CH(CH₃)₂), 1.21 (d, *J* = 6.7 Hz, 3H, CH₃B from 2-CH(CH₃)₂); ¹³C-NMR (DMSO-d⁶), δ, ppm: 159.8 (C₄ Py⁺), 154.2 (C_{2,6} Py⁺), 146.3 (C₁ 1-Ph), 137.8 (C₃ 1-Ph), 131.8 (C₆ 1-Ph), 129.7 (C_{3,5} Py⁺), 128.3 (C₄ 1-Ph), 123.8 (C₅ 1-Ph), 123.6 (C₂ 1-Ph), 31.4 (C₁ i-Pr), 22.0 (C₄ Me), 21.9 (C₂ i-Pr), 21.4 (C₂ i-Pr); ¹⁹F-NMR (DMSO-d⁶), δ, ppm: -70.12 (d, *J* = 712 Hz, PF₆⁻); LC-MS: (C₁₈H₂₅N₂O₂S), exact mass: 333.2; Found: 333.1 (> 97%); Anal (C₁₈H₂₅N₂O₂S⁺ PF₆⁻) requires (%): C 45.19, H 5.27, N 5.86; Found: C 45.26, H 5.37, N 5.92.

2,6-Di-*n*-butyl-4-methyl-1-(3-sulfamoylphenyl)pyridinium hexafluorophosphate (19e): mp 117-120 °C ; Yield 14.2 %; ¹H-NMR (DMSO-d⁶), δ, ppm: 7.94-8.18 (m, 4H, H-2,4,5,6 1-Ph), 7.93 (s, 2H, H-3,5 Py⁺), 7.62 (br. s, 2H, SO₂NH₂), 2.65 (s, 3H, H 4-CH₃), 2.48(t, 4H, H 2, 6-CH₂CH₂CH₂ CH₃), 1.52 (m, 4H, H 2, 6- CH₂CH₂CH₂ CH₃), 1.18 (m- 4H, H 2, 6- CH₂CH₂CH₂CH₃), 0.72 (t, 6H, H 6- CH₂CH₂CH₂CH₃); ¹³C-NMR (DMSO-d⁶), δ, ppm: 159.5 (C₄ Py⁺), 157.8 (C_{2,6} Py⁺), 146.0 (C₁ 1-Ph), 137.2 (C₃ 1-Ph), 131.4 (C₆ 1-Ph), 130.1 (C_{3,5} Py⁺), 128.3 (C₄ 1-Ph), 126.1 (C₅ 1-Ph), 124.1 (C₂ 1-Ph), 33.1 (C₁ n-Bu), 29.8 (C₂ n-Bu), 21.5 (C₄ Me), 21.4 (C₃ n-Bu), 13.2 (C₄ n-Bu) ; ¹⁹F-NMR (DMSO-d⁶), δ, ppm: -70.16 (d, *J* = 712 Hz, PF₆⁻); LC-MS: (C₂₀H₂₉N₂O₂S), exact mass: 361.2; Found: 361.1 (> 97%); Anal (C₂₀H₂₉N₂O₂S⁺ PF₆⁻) requires (%): C 47.43, H 5.77, N 5.53; Found: C 47.65, H 5.85, N 5.62.

2-Ethyl-4,6-dimethyl-1-(3-sulfamoylphenyl)pyridinium hexafluorophosphate (19f): mp 203-207 °C ; Yield 31.5 %; ¹H-NMR (DMSO-d⁶), δ, ppm: 8.11-8.18 (s, 2H, H-3,5 Py⁺), 7.80-8.01 (m, 4H, H-2,4,5,6 1-Ph), 7.62 (br. s, 2H, SO₂NH₂), 3.32 (s, 3H, H 4-CH₃), 2.68 (s, 3H, H 2-CH₃), 2.26 (t, 3H, H 6-CH₂CH₃), 1.14 (t, 2H, H 2-CH₂CH₃); ¹³C-NMR (DMSO-d⁶), δ, ppm: 159.6 (C₄ Py⁺),

158.8 (C₂ Py⁺), 154.6 (C₆ Py⁺), 146.2 (C₁ 1-Ph), 137.8 (C₃ 1-Ph), 131.8 (C₆ 1-Ph), 129.8 (C₅ Py⁺), 128.3 (C₃ Py⁺), 127.1 (C₄ 1-Ph), 125.2 (C₅ 1-Ph), 123.7 (C₂ 1-Ph), 27.1 (C₁ Et), 21.8 (C₄ Me), 21.4 (C₆ Me), 12.0 (C₂ Et); ¹⁹F-NMR (DMSO-d⁶), δ, ppm: -70.15 (d, *J* = 712 Hz, PF₆⁻); LC-MS: (C₁₅H₁₉N₂O₂S), exact mass: 291.1; Found: 291.0 (>97%); Anal (C₁₅H₁₉N₂O₂S⁺ PF₆⁻) requires (%): C 41.29, H 4.39, N 6.42; Found: C 41.11, H 4.33, N 6.48.

2,4-Dimethyl-6-n-propyl-1-(3-sulfamoylphenyl)pyridinium hexafluorophosphate (19g): mp 165-167 °C ; Yield 20.6 %; ¹H-NMR (DMSO-d⁶), δ, ppm: 8.12-8.18 (m, 2H, H-3,5 Py⁺), 7.87-8.00 (m, 4H, H-2,4,5,6 1-Ph), 7.61 (br. s, 2H, SO₂NH₂), 3.34 (s, 3H, H 4-CH₃), 2.65 (s, 3H, H 2-CH₃), 2.29 (m, 2H, H 6-CH₂CH₂CH₃), 1.57 (hex, *J* = 7.5 Hz, 2H, H 6-CH₂CH₂CH₃), 0.82 (t, *J* = 7.3 Hz, 3H, H 6-CH₂CH₂CH₃); ¹³C-NMR (DMSO-d⁶), δ, ppm: 159.4 (C₄ Py⁺), 157.5 (C₂ Py⁺), 154.8 (C₆ Py⁺), 146.2 (C₁ 1-Ph), 137.8 (C₃ 1-Ph), 131.7 (C₆ 1-Ph), 129.8 (C₅ Py⁺), 128.3 (C₃ Py⁺), 127.2 (C₄ 1-Ph), 126.1 (C₅ 1-Ph), 123.8 (C₂ 1-Ph), 35.1 (C₁ n-Pr), 21.8 (C₄ Me), 21.0 (C₆ Me), 13.3 (C₃ n-Pr); ¹⁹F-NMR (DMSO-d⁶), δ, ppm: -70.12 (d, *J* = 711 Hz, PF₆⁻); LC-MS: (C₁₆H₂₁N₂O₂S), exact mass: 305.1; Found: 305.0 (>97%); Anal (C₁₆H₂₁N₂O₂S⁺ PF₆⁻) requires (%): C 42.67, H 4.70, N 6.22; Found: C 42.75, H 4.88, N 6.23.

2-Isopropyl-4,6-dimethyl-1-(3-sulfamoylphenyl)pyridinium hexafluorophosphate (19h): mp 209-215 °C ; Yield 26 %; ¹H-NMR (DMSO-d⁶), δ, ppm: 8.13-8.21 (m, 2H, H-3,5 Py⁺), 7.90-8.06 (m, 4H, H 2, 3, 4, 5 1-Ph), 7.64 (br. s, 2H, SO₂NH₂), 2.67 (s, 3H, H 4-CH₃), 2.59 (hep, *J* = 6.8 Hz, 1H, H 2-CH(CH₃)₂), 2.27 (s, 3H, H 2-CH₃), 1.23 (d, *J* = 6.7 Hz, 3H, H CH₃A from 2-CH(CH₃)₂), 1.21 (d, *J* = 6.7 Hz, 3H, CH₃B from 2-CH(CH₃)₂); ¹³C-NMR (DMSO-d⁶), δ, ppm: 163.2 (C₄ Py⁺),

159.8 (C₂, Py⁺), 154.2 (C₆ Py⁺), 146.3 (C₁ 1-Ph), 137.8 (C₃ 1-Ph), 131.7 (C₆ 1-Ph), 129.7 (C₅ Py⁺), 128.3 (C₃ Py⁺), 127.2 (C₄ 1-Ph), 123.8 (C₅ 1-Ph), 123.6 (C₂ 1-Ph), 31.4 (C₁ i-Pr), 22.0 (C₄ Me), 21.9 (C₆ Me), 21.4 (C₂ i-Pr); ¹⁹F-NMR (DMSO-d⁶), δ, ppm: -70.12 (d, *J* = 712 Hz, PF₆⁻); LC-MS: (C₁₆H₂₁N₂O₂S), exact mass: 305.1; Found: 305.0 (> 97%); Anal (C₁₆H₂₁N₂O₂S⁺ PF₆⁻) requires (%): C 42.67, H 4.70, N 6.22; Found: C 42.88, H 4.74, N 6.34.

2-n-Butyl-4,6-dimethyl-1-(3-sulfamoylphenyl)pyridinium hexafluorophosphate (19i): mp 200-205 °C; Yield 15.5 %; ¹H-NMR (DMSO-d⁶), δ, ppm: 8.13-8.16 (m, 2H, H-3,5 Py⁺), 7.89-7.99 (m, 4H, H-2,4,5,6 1-Ph), 7.63 (br. s, 2H, SO₂NH₂), 3.33 (s, 3H, H 4-CH₃), 2.63 (s, 3H, H 6-CH₃), 2.29 (t, 2H- H, 2- CH₂ CH₂CH₂ CH₃), 1.53 (m, 2H, H 2-CH₂CH₂CH₂ CH₃), 1.18 (m- 2H- H 2- CH₂ CH₂CH₂CH₃), 0.72 (t, 3H, H 6- CH₂CH₂CH₂CH₃); ¹³C-NMR (DMSO-d⁶), δ, ppm: 159.4 (C₄ Py⁺), 157.7 (C₂, Py⁺), 154.7 (C₆ Py⁺), 146.2 (C₁ 1-Ph), 137.8 (C₃ 1-Ph), 131.6 (C₆ 1-Ph), 129.9 (C₅ Py⁺), 128.3 (C₃ Py⁺), 127.2 (C₄ 1-Ph), 126.1 (C₅ 1-Ph), 123.8 (C₂ 1-Ph), 31.4 (C₁ n-Bu), 29.8 (C₄ Me), 25.5 (C₆ Me), 21.8 (C₂ n-Bu), 21.5 (C₃ n-Bu), 13.2 (C₄ n-Bu); ¹⁹F-NMR (DMSO-d⁶), δ, ppm: -70.14 (d, *J* = 711 Hz, PF₆⁻); LC-MS: (C₁₇H₂₃N₂O₂S), exact mass: 319.1; Found: 319.0 (> 97%); Anal (C₁₇H₂₃N₂O₂S⁺ PF₆⁻) requires (%): C 43.97, H 4.99, N 6.03; Found: C 44.01, H 5.02, N 6.07.

2,6-Dimethyl-4-phenyl-1-(3-sulfamoyl-phenyl)-pyridinium hexafluorophosphate (19j): mp 309-312 °C ; Yield 35.6 %; ¹H-NMR (DMSO-d⁶), δ, ppm: 8.54 (br. s, 2H, H-3,5 Py⁺), 8.21 (br. s, H, H 1-Ph), 8.19-8.10 (m, 3H, H-4 1-Ph, H-2,6 4-Ph), 8.02-7.93 (m, 2H, H-5,6 1-Ph), 7.75 (d, *J* = 3.6, 3H, H-3,4,5 4-Ph), 7.61 (br. S, 2H, SO₂NH₂), 3.30 (s, 6H, H 2,6-CH₃); ¹³C-NMR (DMSO-d⁶), δ, ppm: 155.7 (C_{2,6} Py⁺), 155.1 (C₄ Py⁺), 146.3 (C₁ 1-Ph), 138.3 (C₁ 4-Ph), 133.5 (C₃ 1-Ph),

132.2 (C₄ 4-Ph), 131.8 (C₆ 1-Ph), 129.7 (C_{3,5} 4-Ph), 129.5 (C₄ 1-Ph), 128.2 (C₅ 1-Ph), 128.0 (C_{1,6} 4-Ph), 123.4 (C_{3,5} Py⁺), 123.2 (C₂ 1-Ph), 21.9, (C_{2,6} Me); ¹⁹F-NMR (DMSO-d⁶), δ, ppm: -70.15, (d, *J* = 712 Hz, PF₆⁻); LC-MS: (C₁₉H₁₉N₂O₂S), exact mass: 339.1; Found: 339.0 (> 97%); Anal (C₁₉H₁₉N₂O₂S⁺ PF₆⁻) requires (%): C 47.11, H 3.95, N 5.78; Found: C 47.24, H 4.03, N 5.86.

2,6-Diethyl-4-phenyl-1-(3-sulfamoyl-phenyl)-pyridinium hexafluorophosphate (19k): mp 290-293 °C ; Yield 25.4 %; ¹H-NMR (DMSO-d⁶), δ, ppm: 8.38 (br. s, 2H, H-3,5 Py⁺), 8.25 (br. s, H, H-2 1-Ph), 8.22-8.16 (m, 3H, H-4 1-Ph, H-2,6 4-Ph), 7.98-8.01 (m, Hz, 2H, H-5,6 1-Ph), 7.72-7.76 (d, 3H, H-3,4,5 4-Ph), 7.69 (br. S, 2H, SO₂NH₂), 2.65-2.55 (m, 4H, H 2,6-CH₂CH₃), 1.27-1.17 (m, 6H, H 2,6-CH₂CH₃); ¹³C-NMR (DMSO-d⁶), δ, ppm: 160.2 (C_{2,6} Py⁺), 155.7 (C₄ Py⁺), 146.1 (C₁ 1-Ph), 137.3 (C₁ 4-Ph), 133.9 (C₃ 1-Ph), 132.2 (C₄ 4-Ph), 131.6 (C₆ 1-Ph), 130.0 (C_{3,5} 4-Ph), 129.7 (C₄ 1-Ph), 128.4 (C₅ 1-Ph), 128.3 (C_{1,6} 4-Ph), 124.0 (C_{3,5} Py⁺), 121.7 (C₂ 1-Ph), 27.6 (C₁ Et), 12.5 (C₂ Et); ¹⁹F-NMR (DMSO-d⁶), δ, ppm: no signal; LC-MS: (C₂₁H₂₃N₂O₂S), exact mass: 367.1; Found: 367.0 (> 97%); Anal (C₂₁H₂₃N₂O₂S) requires (%): C 49.22, H 4.52, N 5.47; Found: C 49.19, H 4.67, N 5.54.

2,6-Di-n-propyl-4-phenyl-1-(3-sulfamoyl-phenyl)-pyridinium hexafluorophosphate (19l): mp 218-221 °C ; Yield 45.3 %; ¹H-NMR (DMSO-d⁶), δ, ppm: 8.44 (br. s, 2H, H-3,5 Py⁺), 8.18-8.30 (m, 4H, H-2,4 1-Ph, H-2,6 4-Ph), 8.07-7.94 (m, 2H, H-5,6 1-Ph), 7.73-7.79 (m, 3H, H-3,4,5 4-Ph), 7.66 (br. s, 2H, SO₂NH₂), 2.64-2.45 (m, 4H, H 2,6-CH₂CH₂CH₃), 1.66-1.60 (m, 4H, H 2,6-CH₂CH₂CH₃), 0.88-0.75 (m, 6H, H 2,6-CH₂CH₂CH₃); ¹³C-NMR (DMSO-d⁶), δ, ppm: 158.8 (C_{2,6} Py⁺), 155.2 (C₄ Py⁺), 146.0 (C₁ 1-Ph), 137.2 (C₁ 4-Ph), 133.7 (C₃ 1-Ph), 132.2 (C₄ 4-Ph), 131.3

(C₆ 1-Ph), 130.0 (C_{3,5} 4-Ph), 129.6 (C₄ 1-Ph), 128.3 (C₅ 1-Ph), 128.2 (C_{1,6} 4-Ph), 124.0 (C_{3,5} Py⁺), 122.4 (C₂ 1-Ph), 35.6 (C₁ n-Pr), 21.4 (C₂ n-Pr), 13.4 (C₃ n-Pr); ¹⁹F-NMR (DMSO-d⁶), δ, ppm: -77.86 (d, *J* = 792 Hz, PF₆⁻); LC-MS: (C₂₃H₂₇N₂O₂S), exact mass: 395.2; Found: 395.1 (> 97%); Anal (C₂₃H₂₇N₂O₂S⁺ PF₆⁻) requires (%): C 51.11, H 5.04, N 5.18; Found: C 51.34, H 5.23, N 5.28.

2,6-Diisopropyl-4-phenyl-1-(3-sulfamoylphenyl)pyridinium hexafluorophosphate (19m): mp 261-263 °C; Yield 38.7 %; ¹H-NMR (DMSO-d⁶), δ, ppm: 8.41 (s, 2H, H-3,5 Py⁺), 8.15-8.32 (m, 4H, H-2,4,5,6 1-Ph), 7.70-8.00 (m, 5H, H 4-Ph), 7.66 (br. s, 2H, SO₂NH₂), 3.33 (m, 2H, H 2,4 -CH(CH₃)₂), 1.32 (d, 12H, H 2,4 -CH(CH₃)₂), ¹³C-NMR (DMSO-d⁶), δ, ppm: 164.1 (C₄ Py⁺), 156.2 (C_{2,6} Py⁺), 146.3 (C₁ 1-Ph), 137.5 (C₃ 1-Ph), 134.0 (C_{3,5} 4-Ph), 132.1 (C_{2,6} 4-Ph), 131.6 (C₄ 4-Ph), 129.8 (C₆ 1-Ph), 129.6 (C₄ 1-Ph), 128.5 (C₅ 1-Ph), 123.6 (C_{3,5} Py⁺), 120.2 (C₂ 1-Ph), 32.2 (C₁ i-Pr), 21.8 (C₂ i-Pr), 21.7 (C₂ i-Pr); ¹⁹F-NMR (DMSO-d⁶), δ, ppm: -70.15 (d, *J* = 712 Hz, PF₆⁻); LC-MS: (C₂₃H₂₇N₂O₂S), exact mass: 395.2; Found: 395.1 (> 97%); Anal (C₂₃H₂₇N₂O₂S⁺ PF₆⁻) requires (%): C 51.11, H 5.04, N 5.18; Found: C 51.19, H 5.09, N 5.30.

2,6-Di-n-butyl-4-phenyl-1-(3-sulfamoyl-phenyl)-pyridinium hexafluorophosphate (19n): mp 181-184 °C ; Yield 25.3 %; ¹H-NMR (DMSO-d⁶), δ, ppm: 8.45 (br. s, 2H, H-3,5 Py⁺), 8.19-8.25 (m, 4H, H-2,4 1-Ph, H-2,6 4-Ph), 8.09-7.96 (m, 2H, H-5,6 1-Ph), -7.65-7.74 (m, 3H, H-3,4,5 4-Ph), 7.75 (br. S, 2H, SO₂NH₂), 2.67-2.60 (m, 4H, H 2,6- CH₂ CH₂CH₂ CH₃), 1.64-1.51 (m, 4H, H 2,6-CH₂CH₂CH₂ CH₃), 1.25-1.15 (m, 4H, H 2,6- CH₂ CH₂CH₂CH₃), 0.79-0.69 (m, 6H, H 2,6-CH₂CH₂CH₂CH₃); ¹³C-NMR (DMSO-d⁶), δ, ppm: 159.1 (C_{2,6} Py⁺), 155.3 (C₄ Py⁺), 146.1 (C₁ 1-Ph), 137.2 (C₁ 4-Ph), 133.7 (C₃ 1-Ph), 132.2 (C₄ 4-Ph), 131.2 (C₆ 1-Ph), 130.1 (C_{3,5} 4-Ph), 129.7

(C₄ 1-Ph), 128.3 (C₅ 1-Ph), 124.2 (C_{1,6} 4-Ph), 124.0 (C_{3,5} Py⁺), 122.5 (C₂ 1-Ph), 33.5 (C₁ n-Bu), 30.1 (C₂ n-Bu), 21.6 (C₃ n-Bu), 13.2 (C₄ n-Bu); ¹⁹F-NMR (DMSO-d⁶), δ, ppm: -76.83 (d, *J* = 780 Hz, PF₆⁻); LC-MS: (C₂₅H₃₁N₂O₂S), exact mass: 423.2; Found: 423.1 (> 97%); Anal (C₂₅H₃₁N₂O₂S⁺ PF₆⁻) requires (%): C 52.81, H 5.50, N 4.93; Found: C 52.78, H 5.48, N 5.05.

2-Methyl-4,6-diphenyl-1-(3-sulfamoyl-phenyl)-pyridinium hexafluorophosphate (19o): mp 143-147 °C ; Yield 35.5 %; ¹H-NMR (DMSO-d⁶), δ, ppm: 8.76 (br. s, H, H-3 Py⁺), 8.50 (br. s, H, H-3 Py⁺), 8.26 (d, *J* = 2.0 Hz, 2H, H- 2,6 2-Ph), 8.21 (t, *J* = 1.8 Hz, H, H-2 1-Ph), 7.78 (d, *J* = 0.8 Hz, H, H-6 2-Ph), 7.73 (d, *J* = 6.6 Hz, H, H-4 2-Ph), 7.70- 7.65 (m, 4H, H-4,6 1-Ph, H-3,5 2-Ph), 7.58 (br. S, 2H, SO₂NH₂), 7.42-7.31 (m, 5H, H-2,3,4,5,6 4-Ph), 1.14-1.06 (s, 3H, 2-CH₃); ¹³C-NMR (DMSO-d⁶), δ, ppm: 156.1 (C₂ Py⁺), 155.9 (C₄ Py⁺), 155.3 (C₆ Py⁺), 145.3 (C₁ 1-Ph), 138.7 (C₁ 4-Ph), 133.3 (C₃ 1-Ph), 132.5 (C₁ 6-Ph), 132.4 (C₅ 4-Ph), 130.7 (C₃ 4-Ph), 130.4 (C_{2,6} 4-Ph), 129.9 (C₄ 4-Ph), 129.7 (C₄ 6-Ph), 129.6 (C_{2,6} 6-Ph), 128.4 (C_{3,5} 6-Ph), 128.1 (C₆ 1-Ph), 127.5 (C₄ 1-Ph), 124.8 (C₅ 1-Ph), 123.7 (C₂ 1-Ph), 22.2, (C₁ Me); ¹⁹F-NMR (DMSO-d⁶), δ, ppm: -78.25 (d, *J* = 951.5 Hz, PF₆⁻); LC-MS: (C₂₄H₂₁N₂O₂S), exact mass: 401.1; Found: 401.0 (> 97%); Anal (C₂₄H₂₁N₂O₂S⁺ PF₆⁻) requires (%): C 52.75, H 3.87, N 5.13; Found: C 52.84, H 4.01, N 5.23.

2-Ethyl-4,6-diphenyl-1-(3-sulfamoyl-phenyl)-pyridinium hexafluorophosphate (19p): mp 118-122 °C ; Yield 38.5 %; ¹H-NMR (DMSO-d⁶), δ, ppm: 8.62 (br. s, H, H-3 Py⁺), 8.49 (br. s, H, H-5 Py⁺), 8.34-8.26 (m, 2H, H-2,6 2-Ph), 8.24 (br. s, H, H-2 1-Ph), 7.87 (d, *J* = 14.3 Hz, H, H-6 2-Ph), 7.81 (d, *J* = 13.6 Hz, H, H-4 2-Ph), 7.75- 7.66 (m, 4H, H-4,6 1-Ph, H-3,5 2-Ph), 7.64 (br. S, 2H, SO₂NH₂), 7.45-7.30 (m, 5H, H-2,3,4,5,6 4-Ph), 2.81-2.69 (m, 2H, H 2-CH₂CH₃), 1.28-1.09

(m, 3H, H 2-CH₂CH₃); ¹³C-NMR (DMSO-d₆), δ, ppm: 160.4 (C₂ Py⁺), 156.0 (C₄ Py⁺), 155.6 (C₆ Py⁺), 145.1 (C₁ 1-Ph), 138.1 (C₁ 4-Ph), 133.5 (C₃ 1-Ph), 132.6 (C₁ 6-Ph), 132.3 (C₅ 4-Ph), 130.7 (C₃ 4-Ph), 130.4 (C_{2,6} 4-Ph), 129.8 (C₄ 4-Ph), 129.6 (C₄ 6-Ph), 128.5 (C_{2,6} 6-Ph), 128.0 (C_{3,5} 6-Ph), 127.6 (C₆ 1-Ph), 125.1 (C₄ 1-Ph), 123.7 (C₅ 1-Ph), 123.0 (C₂ 1-Ph), 27.6 (C₁ Et), 12.7 (C₂ Et); ¹⁹F-NMR (DMSO-d₆), δ, ppm: -78.25 (d, *J* = 951.3 Hz, PF₆⁻); LC-MS: (C₂₅H₂₃N₂O₂S), exact mass: 415.1; Found: 415.0 (> 97%); Anal (C₂₅H₂₃N₂O₂S⁺ PF₆⁻) requires (%): C 53.57, H 4.14, N 5.00; Found: C 53.68, H 4.22, N 5.07.

2-n-Propyl-4,6-diphenyl-1-(3-sulfamoyl-phenyl)-pyridinium hexafluorophosphate (19r): mp 135-138 °C ; Yield 25.4 %; ¹H-NMR (DMSO-d₆), δ, ppm: 8.66 (br. s, d, H, H-3 Py⁺), 8.49 (br. s, H, H-5 Py⁺), 8.30 (d, *J* = 23.2 Hz, H, H-2 2-Ph), 8.27 (d, *J* = 23.2 Hz, H, H-6 2-Ph), 8.24 (t, *J* = 1.7 Hz, H, H-2 1-Ph), 7.83 (d, *J* = 0.9 Hz, H, H-6 2-Ph), 7.81 (d, *J* = 0.96 Hz, H, H-4 2-Ph), 7.75-7.64 (m, 4H, H-4,6 1-Ph, H-3,5 2-Ph), 7.61 (br. s, 2H, SO₂NH₂), 7.48-7.29 (m, 5H, H-2,3,4,5,6 4-Ph), 2.80-2.64 (m, 2H, H 2-CH₂CH₂CH₃), 1.71-1.61 (m, 2H, H 2-CH₂CH₂CH₃), 0.92-0.78 (m, 3H, H 2-CH₂CH₂CH₃); ¹³C-NMR (DMSO-d₆), δ, ppm: 159.0 (C₂ Py⁺), 156.1 (C₄ Py⁺), 155.4 (C₆ Py⁺), 145.0 (C₁ 1-Ph), 138.1 (C₁ 4-Ph), 133.4 (C₃ 1-Ph), 132.7 (C₁ 6-Ph), 132.4 (C₅ 4-Ph), 130.7 (C₃ 4-Ph), 130.3 (C_{2,6} 4-Ph), 129.8 (C₄ 4-Ph), 129.7 (C₄ 6-Ph), 129.6 (C_{2,6} 6-Ph), 128.5 (C_{3,5} 6-Ph), 127.6 (C₆ 1-Ph), 125.1 (C₄ 1-Ph), 123.8 (C₅ 1-Ph), 123.7 (C₂ 1-Ph), 35.6 (C₁ n-Pro), 21.6 (C₂ n-Pro), 13.5 (C₃ n-Pro) ; ¹⁹F-NMR (DMSO-d₆), δ, ppm: -78.23 (d, *J* = 951.8 Hz, PF₆⁻); LC-MS: (C₂₆H₂₅N₂O₂S), exact mass: 429.2; Found: 429.1 (> 97%); Anal (C₂₆H₂₅N₂O₂S⁺ PF₆⁻) requires (%): C 54.35, H 4.39, N 4.88; Found: C 54.43, H 4.46, N 4.90.

2-Isopropyl-4,6-diphenyl-1-(3-sulfamoyl-phenyl)-pyridinium hexafluorophosphate (19q):

mp 146-148 °C ; Yield 18.4 %; ¹H-NMR (DMSO-d⁶), δ, ppm: 8.65 (br. s, H, H-3 Py⁺), 8.46 (br. s, H, H-5 Py⁺), 8.32 (d, *J* = 6.5 Hz, 2H, H-2,6 2-Ph), 8.27 (br. s, H, H-2 1-Ph), 7.87 (d, *J* = 7.3 Hz, H, H-6 2-Ph), 7.86 (d, *J* = 6.8 Hz, H, H-4 2-Ph), 7.79- 7.69 (m, 4H, H-4,6 1-Ph, H-3,5 2-Ph), 7.67 (br. s, 2H, SO₂NH₂), 7.46-7.30 (m, 5H, H-2,3,4,5,6 4-Ph), 2.79-2.74 (m, H, H 2-CH(CH₃)₂), 1.43-1.30 (m, 6H, H 2-CH(CH₃)₂); ¹³C-NMR (DMSO-d⁶), δ, ppm: 164.8 (C₂ Py⁺), 155.9 (C₄ Py⁺), 155.7 (C₆ Py⁺), 145.2 (C₁ 1-Ph), 138.2 (C₁ 4-Ph), 133.6 (C₃ 1-Ph), 133.0 (C₁ 6-Ph), 132.4 (C₅ 4-Ph), 130.7 (C₃ 4-Ph), 129.8 (C_{2,6} 4-Ph), 129.7 (C₄ 4-Ph), 129.6 (C₄ 6-Ph), 128.7 (C_{2,6} 6-Ph), 128.0 (C_{3,5} 6-Ph), 127.7 (C₆ 1-Ph), 125.6 (C₄ 1-Ph), 123.9 (C₅ 1-Ph), 121.1 (C₂ 1-Ph), 32.2 (C₁ i-Pr), 21.8 (C₂ i-Pr), 21.7 (C₂ i-Pr); ¹⁹F-NMR (DMSO-d⁶), δ, ppm: -70.14 (d, *J* = 712 Hz, PF₆⁻); LC-MS: (C₂₆H₂₅N₂O₂S), exact mass: 429.2; Found: 429.1 (> 97%); Anal (C₂₆H₂₅N₂O₂S⁺ PF₆⁻) requires (%): C 54.35, H 4.39, N 4.88; Found: C 54.37, H 4.46, N 4.92.

2-n-Butyl-4,6-diphenyl-1-(3-sulfamoyl-phenyl)-pyridinium hexafluorophosphate (19s): mp

143-147 °C ; Yield 15.7 %; ¹H-NMR (DMSO-d⁶), δ, ppm: 8.67 (br. s, H, H-3 Py⁺), 8.48 (br. s, H, H-5 Py⁺) 8.28 (d, *J* = 7.9 Hz, 2H, H-2,6 2-Ph), 8.23 (br. s, H, H-2 1-Ph), 7.87 (d, *J* = 7.8 Hz, H, H-6 2-Ph), 7.81 (d, *J* = 7.9 Hz, H, H-4 2-Ph), 7.75- 7.63 (m, 4H, H-4,6 1-Ph, H-3,5 2-Ph), 7.59 (br. s, 2H, SO₂NH₂), 7.43-7.30 (m, 5H, H-2,3,4,5,6 4-Ph), 2.79-2.69 (m, 2H, H 2- CH₂ CH₂CH₂ CH₃), 1.66-1.59 (m, 2H, H 2-CH₂CH₂CH₂CH₃), 1.25-1.18 (m, 2H, H 2- CH₂ CH₂CH₂CH₃), 0.78-0.68 (m, 3H, H 2- CH₂CH₂CH₂CH₃); ¹³C-NMR (DMSO-d⁶), δ, ppm: 159.4 (C₂ Py⁺), 156.1 (C₄ Py⁺), 155.5 (C₆ Py⁺), 145.1 (C₁ 1-Ph), 138.2 (C₁ 4-Ph), 133.5 (C₃ 1-Ph), 132.8 (C₁ 6-Ph), 132.4 (C₅ 4-Ph), 130.8 (C₃ 4-Ph), 130.4 (C_{2,6} 4-Ph), 129.9 (C₄ 4-Ph), 129.8 (C₄ 6-Ph), 129.7 (C_{2,6} 6-Ph), 128.5 (C_{3,5} 6-Ph), 128.1 (C₆ 1-Ph), 127.6 (C₄ 1-Ph), 125.2 (C₅ 1-Ph), 123.8 (C₂ 1-Ph), 33.5 (C₁ n-Bu),

30.3 (C₂ n-Bu), 21.7 (C₃ n-Bu), 13.2 (C₄ n-Bu) ; ¹⁹F-NMR (DMSO-d⁶), δ, ppm: -70.15 (d, *J* = 712 Hz, PF₆⁻); LC-MS: (C₂₇H₂₇N₂O₂S), exact mass: 443.2; Found: 443.1 (> 97%); Anal (C₂₇H₂₇N₂O₂S⁺ PF₆⁻) requires (%): C 55.10, H 4.62, N 4.76; Found: C 55.34, H 4.78, N 4.88.

2,3,4,6-Tetramethyl-1-(3-sulfamoylphenyl)pyridinium hexafluorophosphate (19t): mp 215-217 °C; Yield 18.7 %; ¹H-NMR (DMSO-d⁶), δ, ppm: 7.92 (s, 2H, H-5 Py⁺), 7.82-8.13 (m, 4H, H-2,4,5,6 1-Ph), 7.53 (br. s, 2H, SO₂NH₂), 2.60 (s, 3H, H 4-CH₃), 2.39 (s, 3H, H 3-CH₃), 2.28 (s, 3H, H 6-CH₃), 2.25 (s, 3H, H 2-CH₃) ; ¹³C-NMR (DMSO-d⁶), δ, ppm: 157.7 (C₄ Py⁺), 153.0 (C₂, Py⁺), 151.1 (C₆ Py⁺), 146.4 (C₁ 1-Ph), 139.3 (C₃ 1-Ph), 133.9 (C₆ 1-Ph), 131.9 (C₅ Py⁺), 129.5 (C₃ Py⁺), 128.1 (C₄ 1-Ph), 127.1 (C₅ 1-Ph), 123.5 (C₂ 1-Ph), 21.6 (C₄ Me), 20.9 (C₂ Me), 19.4 (C₆ Me), 15.3 (C₅ Me); ¹⁹F-NMR (DMSO-d⁶), δ, ppm: -70.15 (d, *J* = 712 Hz, PF₆⁻); LC-MS: (C₁₅H₁₉N₂O₂S), exact mass: 291.1; Found: 291.0 (> 97%); Anal (C₁₅H₁₉N₂O₂S⁺ PF₆⁻) requires (%): C 41.29, H 4.39, N 6.42; Found: C 41.43, H 4.44, N 6.50.

2,6-Dimethyl-3,5-(1,9-nonane-diyl)-1-(3-sulfamoyl-phenyl)pyridinium hexafluorophosphate (19u): mp 183-186 °C ; Yield 68 %; ¹H-NMR (DMSO-d⁶), δ, ppm: 8.64 (br. s, 2H, H-3,5 Py⁺), 8.19 (br. s, 1H, H-4 Py⁺), 8.15 (d, *J* = 8.2 Hz, H, H-2 1-Ph), 7.98 (dd, *J*₁ = 8.0 Hz, *J*₂ = 7.9 Hz, 2H, H-4,6 1-Ph), 7.84 (d, *J* = 8.9 Hz, H, H-5 1-Ph), 7.60 (br. s, 2H, SO₂NH₂), 2.97 (t, *J* = 6.0 Hz, 4H, H-1,9 cyclo), 1.76-1.69 (m, 4H, H-2,8 cyclo), 1.25-1.03 (m, 10H, H-3,4,5,6,7 cyclo); ¹³C-NMR (DMSO-d⁶), δ, ppm: 152.0 (C_{3,5} Py⁺), 147.9 (C₁ 1-Ph), 146.3 (C₄ Py⁺), 139.7 (C₃ 1-Ph), 136.5 (C_{2,6} Py⁺), 131.9 (C₆ 1-Ph), 129.5 (C₄ 1-Ph), 128.1 (C₅ 1-Ph), 123.5 (C₂ 1-Ph), 30.8 (C_{1,9} cyclo), 25.5 (C_{2,8} cyclo), 24.5 (C₃ cyclo), 23.9 (C₇ cyclo), 18.6 (C_{4,5,6} cyclo); ¹⁹F-NMR (DMSO-d⁶), δ, ppm: -

70.1 (d, $J = 712$ Hz, PF_6^-); LC-MS: ($\text{C}_{22}\text{H}_{31}\text{N}_2\text{O}_2\text{S}$), exact mass: 387.2; Found: 387.1 (> 97%); Anal ($\text{C}_{22}\text{H}_{31}\text{N}_2\text{O}_2\text{S}^+ \text{PF}_6^-$) requires (%): C 49.62, H 5.87, N 5.26; Found: C 49.78, H 5.95, N 5.33.

2,4-Dimethyl-6-phenyl-1-(3-sulfamoylphenyl)pyridinium hexafluorophosphate (19v): mp 153-154 °C; Yield 20.2 %; $^1\text{H-NMR}$ (DMSO-d_6), δ , ppm: 8.15 (br.s, 2H, H-3,5 Py^+), 8.14 (m, 1H, H-2 1-Ph), 7.83-7.92 (m, 1H, H-6 1-Ph), 7.62-7.74 (m, 2H, H-4 1-Ph), 7.52 (br. s, 2H, SO_2NH_2), 7.29-7.38 (m, 5H, H 6-Ph), 2.67 (s, 3H, H 4- CH_3), 2.42 (s, 3H, H 2- CH_3); $^{13}\text{C-NMR}$ (DMSO-d_6), δ , ppm: 159.8 ($\text{C}_4 \text{Py}^+$), 155.0 (C_2, Py^+), 154.8 ($\text{C}_6 \text{Py}^+$), 145.4 (C_1 1-Ph), 138.7 (C_3 1-Ph), 132.4 (C_2 2-Ph), 130.7 (C_6 2-Ph), 130.5 (C_3 2-Ph), 130.0 (C_5 2-Ph), 129.5 (C_4 2-Ph), 128.6 ($\text{C}_5 \text{Py}^+$), 128.2 ($\text{C}_3 \text{Py}^+$), 127.9 (C_1 2-Ph), 127.6 (C_4 1-Ph), 124.9 (C_2 1-Ph), 21.9 (C_4 Me), 21.3 (C_6 Me); $^{19}\text{F-NMR}$ (DMSO-d_6), δ , ppm: -70.22 (d, $J = 712$ Hz, PF_6^-); LC-MS: ($\text{C}_{19}\text{H}_{19}\text{N}_2\text{O}_2\text{S}$), exact mass: 339.1; Found: 339.0 (> 97%); Anal ($\text{C}_{19}\text{H}_{19}\text{N}_2\text{O}_2\text{S}^+ \text{PF}_6^-$) requires (%): C 47.11, H 3.95, N 5.78; Found: C 47.32, H 4.06, N 5.83.

4-Methyl-2,6-diphenyl-1-(3-sulfamoylphenyl)pyridinium hexafluorophosphate (19w): mp 230-233 °C ; Yield 19.3 %; $^1\text{H-NMR}$ (DMSO-d_6), δ , ppm: 8.23 (br. s, 2H, H-3,5 Py^+), 7.99 (br. s, 1H, H-2 1-Ph), 7.60 (m, 2H, H-4,6 1-Ph), 7.45 (br.s, 2H, SO_2NH_2), 7.40-7.30 (m, 11H, H-2,3,4,5,6-2,6-Ph, H-5 1-Ph), 2.79 (t, $J = 20.0$ Hz, 3H, H-4- CH_3); $^{13}\text{C-NMR}$ (DMSO-d_6), δ , ppm: : 160.2 ($\text{C}_4 \text{Py}^+$), 154.8 ($\text{C}_{2,6} \text{Py}^+$), 144.3 (C_1 1-Ph), 138.9 (C_3 1-Ph), 132.4 (C_4 2,6-Ph), 131.4 (C_6 1-Ph), 130.0 ($\text{C}_{3,5} \text{Py}^+$), 129.4 ($\text{C}_{2,6}$ 2,6-Ph), 129.2 (C_4 1-Ph), 128.2 ($\text{C}_{3,5}$ 2,6-Ph), 126.8 (C_5 1-Ph), 125.1 (C_2 1-Ph), 21.3 (C_4 Me); $^{19}\text{F-NMR}$ (DMSO-d_6), δ , ppm: -70.13 (d, $J = 711$ Hz, PF_6^-); LC-MS:

(C₂₄H₂₁N₂O₂S), exact mass: 401.1; Found: 401.0 (> 97%); Anal (C₂₄H₂₁N₂O₂S⁺ PF₆⁻) requires (%): C 52.75, H 3.87, N 5.13; Found: C 52.88, H 4.01, N 5.23.

2,4,6-Triphenyl-1-(3-sulfamoylphenyl)pyridinium hexafluorophosphate (19x): mp 176-180 °C ; Yield 48 %; ¹H-NMR (DMSO-d⁶), δ, ppm: 8.69 (br. s, 2H, H-3,5 Py⁺), 8.37 (d, *J* = 6.9 Hz, 2H, H-4,6 1-Ph), 8.03 (br. s, H, H-2 1-Ph), 7.71-7.59 (m, 5H, H-5 Py⁺, H-2,6 2,6-Ph), 7.46-7.45 (m, 4H, H-3,5 2,9-Ph), 7.44 (br. S, 2H, SO₂NH₂), 7.41-7.31 (m, 7H, H-2,3,4,5,6- 4-Ph, H-4 2,6-Ph); ¹³C-NMR (DMSO-d⁶), δ, ppm: 156.2 (C_{2,6} Py⁺), 155.8 (C₄ Py⁺), 144.4 (C₁ 1-Ph), 139.1 (C₃ 1-Ph), 133.1 (C₁ 4-Ph), 132.7 (C_{3,5} Py⁺), 132.6 (C₆ 1-Ph), 131.5 (C_{3,5} 4-Ph), 130.1 (C_{2,6} 2,6-Ph), 129.7 (C₁ 2,6-Ph), 129.4 (C₄ 2,6-Ph), 128.8 (C_{3,5} 2,6-Ph), 126.9 (C₅ 1-Ph), 126.2 (C₂ 1-Ph), 125.0 (C₄ 2,6-Ph); ¹⁹F-NMR (DMSO-d⁶), δ, ppm: -78.3 (d, *J* = 951.2 Hz, PF₆⁻); LC-MS: (C₂₉H₂₃N₂O₂S), exact mass: 463.1; Found: 463.0 (> 97%); Anal (C₂₉H₂₃N₂O₂S⁺ PF₆⁻) requires (%): C 57.24, H 3.81, N 4.60; Found: C 57.37, H 4.03, N 4.67.

Carbonic Anhydrase Inhibition Assays

The compounds synthesized were assayed as inhibitors of four physiologically relevant CA isoforms, namely the transmembrane tumor associated hCA IX and hCA XII and the off-target cytosolic hCA I and hCA II, using the CO₂ hydrase assay [79]. An Applied Photophysics stopped-flow instrument was used for assaying the CA catalyzed CO₂ hydration activity [80]. Phenol red (at a concentration of 0.2 mM) was used as indicator, working at the absorbance maximum of 557 nm, with 10 mM Hepes (pH 7.5) as buffer, 0.1 M Na₂SO₄ (for maintaining constant ionic strength), following the CA-catalyzed CO₂ hydration reaction for a period of 10 s at 25°C. The CO₂

concentrations ranged from 1.7 to 17 mM for the determination of the kinetic parameters and activation constants. For each inhibitor at least six traces of the initial 5-10% of the reaction have been used for determining the initial velocity. The uncatalyzed rates were determined in the same manner and subtracted from the total observed rates. Stock solutions of inhibitors (10 mM) were prepared in distilled-deionized water and dilutions up to 0.001 μ M were done thereafter with distilled-deionized water. The inhibitor and enzyme solutions were preincubated together for 15 min (standard assay at room temperature prior to assay, to allow for the formation of the E-I complex. The activation constant (K_i) was subsequently obtained from Michaelis-Menten equation, which has been fitted by non-linear least squares using software PRISM 3. Typical inhibition curves are presented in the Supplemental Material. The enzyme concentrations in the assay system were of 12.1 nM for hCA I, of 7.5 nM for hCA II, of 10.5 nM for hCA IX and of 11.9 nM for hCA XII. All enzymes were recombinant ones, obtained as described earlier [10, 71-74]. A brief example of the cloning is presented below for isoform hCA IX. Recombinant hCA IX was produced using the baculovirus-insect cell expression system [10]. A full-length cDNA encoding the catalytic part of CA IX was amplified by PCR using the mouse cDNA clone (I.M.A.G.E Consortium, Accession number BC034412, MRC Geneservice, Cambridge, U.K.) as a template and a synthetic primer set hCA9 (5'-GGCCAGATCTATGTTGTTCTCCGCCCTCCTGCTGGAGGTGATTTG-3') and hCA14R (5'-CGCCGTCGACTTAATGGTGGTGGTGGTGGGAACCACGGGGCACCAGCATTT CACCTGTGGTA-3') (Biomers) that incorporated desired restriction sites, BglII and Sall (underlined), at the 5'-ends, respectively. The obtained PCR product was digested and directionally ligated to BamHI/Sall double digested expression vector pFastBac1. The ligated plasmid was transformed into *E. coli* TOP10 competent cells and the nucleotide sequence of hCA9 gene was

verified by DNA sequencing. The recombinant pFastBac1-hCA9 plasmid was then transformed *E. coli* DH10Bac competent cells for transposition into the bacmid. The successful transposition was confirmed by blue/white screening and the recombinant bacmid DNA was isolated using the PureLink™ HiPure Plasmid purification kit (Invitrogen). PCR analysis using the recombinant bacmid as template source and the primers M13/pUC forward (5'-CCCAGTCACGACGTTGTAAAACG-3') and reverse (5'-AGCGGATAACAATTTACACAGG-3') amplification primer was performed to verify once more successful transposition to the bacmid. The recombinant baculovirus harboring the hCA9 gene was produced by transfecting the recombinant bacmid DNA to *Spodoptera frugiperda*-derived Sf9 cells using CellFECTIN® Reagent (Invitrogen) as described by the manufacturer. Proteins were purified to homogeneity by Ni²⁺-based chromatography; the His-tag was removed by the proteins utilizing a protease site that was included in the sequences. hCA IX as further purified by size exclusion chromatography. Protein purity and homogeneity was assessed by SDS-PAGE in reducing and non-reducing conditions, and by LC-ESI-IT-MS analysis as described earlier [10, 71-74].

Molecular Docking

Three-dimensional structures of the ligands were generated using CORINA 4.2.0 (Molecular Networks GmbH, Germany and Altamira, LLC, USA) with the sulfonamide group deprotonated, which is the appropriate form for the coordination to zinc. Molecular docking calculations were performed using the GOLD software [81] from the CCDC_2020 suite, and the GoldScore scoring function. The structures 6f3b (hCA I) [82], 1ze8 (hCA II) [58], 6rqq (hCA IX)

[83] and 5msa (hCA XII) were used as receptors, with the active site was defined in each case as a sphere with 20 Å diameter around the zinc ion. All other parameters had default values.

Viability assays for measuring the cytotoxicity of novel CAIs in normoxic and hypoxic conditions [45]

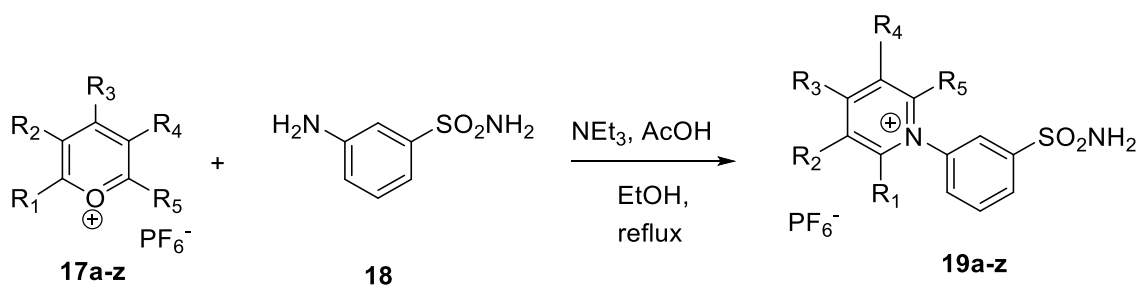
Three cancer cell lines, namely colon (HT-29), ovarian (SKOV3) and breast (MDA-MB-231) carcinomas were used in the study. HT-29 cells were cultured using RPMI media with 10% fetal bovine serum (FBS), while McCoy's media (10% FBS) and DMEM media (10% FBS) were used for SKOV3 line and for MDA-MB231 cell line, respectively.

In a typical experiment, cells were plated in 96 well plates at density of 10,000 cells/well and were allowed to attach and to grow in normal conditions (37 °C, 5% CO₂ in air). Two 96 well plates were prepared from each cell line (one normoxic and another one to be subjected to a hypoxic environment). The hypoxia-designated plates, after 24 h growth in normal conditions, were placed in a hypoxic chamber purged and filled with a low oxygen gas mixture (1% O₂, 5% CO₂ and 94% N₂). After hypoxia induction the closed chamber with hypoxic plates was kept in the incubator at 37 °C for 24 h. Normoxic plates were kept in the same incubator in normal conditions. After 24 h media was aspirated from all plates and cells were treated with CAIs solutions in media containing 10% FBS at 3 different concentrations (1 mM, 100 µM), with each experiment being done in triplicate. A control was made from 4-8 wells of the same cells that received only media with 10% FBS. Hypoxic plates were placed into the hypoxic chamber, which was re-purged and refilled with low oxygen gas mixture, then the closed chamber with plates was returned to the incubator. Normoxic plates were incubated in parallel in the same incubator in air

with 5% CO₂. After another 48 h the normoxic and hypoxic plates were collected, and media was aspirated off. Cells were washed once with PBS, which was subsequently removed, and treated with an MTT solution in media. Typically, a volume of 120 μL solution (made out from MTT 5 mg/mL concentration in PBS diluted 1:6 with the corresponding media) was added to each well and the plates were returned to the incubator for 4 h. The MTT solution was carefully aspirated off and 150 μL of DMSO was added to solubilize the blue formazan crystals, at 37 °C for 5 min. The amount of formazan generated was quantified spectrophotometrically, measuring the absorbance at 570 nm, with a reference absorbance at 690 nm that was subtracted from all readings. Data was reported as the average of three experiments, with one standard deviation from the average value.

Results and discussion

The series of pyridinium sulfonamides **19** was synthesized by direct condensation of pyrylium salts **17** (as hexafluorophosphates) with 3-aminobenzenesulfonamide **18**, in ethanol at reflux, in the presence of triethylamine and acetic acid as catalysts (Scheme 1).



Scheme 1. Synthesis of new pyridinium 3-aminobenzene sulfonamide series via condensation of 3-aminobenzenesulfonamide with pyrylium salts

The substituting moieties of the pyridinium ring of compounds **19** comprise alkyl, aryl, and alkenyl moieties. We started with the compact methyl ones, and iterated towards the bulkier ethyl, n-propyl, iso-propyl, butyl, ending with the much larger phenyl moieties. Combinations of different such substituents were also considered in order to efficiently sample the steric constraints of amphiphilic site P2 (Table 1). The isolated yields of the condensation varied from 14 to 68% and depended highly on the structure of the pyrylium salts used, as expected. One can notice that pyrylium salts having methyl groups in the alpha position of the heterocyclic system were converted into corresponding pyridinium salts with significantly smaller yields as compared with their congeners having long alkyl or aryl substituents in positions 2 and 6, due to a known secondary C-cyclization instead of the desired N-cyclization process [67-69]. Even for these representatives the yields were just fair since the nucleophilicity of the aromatic amine is quite low.

Carbonic Anhydrase Inhibition Assays

The series of 24 compounds of type **19** synthesized in this section were assayed as inhibitors of four physiologically relevant human CA isoforms, including tumor-associated hCA IX and hCA XII and off-target cytosolic hCA I and hCA II, using the CO₂ hydration assay. Acetazolamide (AAZ) was used as standard in these measurements for comparison reasons. The results are presented in Table 1. As one may observe while examining the data from Table 1, pyridinium benzenesulfonamides **19** proved to be very potent inhibitors of tumor-overexpressed CA IX and CA XII, with most of the compounds reaching low nanomolar levels of inhibition, about one order of magnitude lower than acetazolamide standard, thus confirming the validity of

our design. The affinity of these compounds for off-target isozymes CA I and CA II was slightly lower as compared to the targeted isozymes, with CA I being less sensitive to inhibition with these sulfonamides as compared with CA II (Table 1).

Focusing on the membrane-bound isozymes, the most potent compounds against CA IX were the ones bearing pyridinium rings substituted with methyl and phenyl substituents such as **19a**, **19j** and **19o**. These compounds proved also the most potent against CA XII, the two isozymes having in fact a very similar susceptibility for pyridinium sulfonamides **19**, which recommends them as ideal agents for simultaneous inhibition of these tumor-overexpressed enzymes. The substitution pattern proved highly important, with the bulkier phenyl groups being accommodated best in positions 2 and 4 of the pyridinium ring. The 2,6-diphenyl substitution (e.g in **19w**, **19x**) reduced the potency, probably due to increased steric of these substituents. This pattern was generally valid, with a reduced potency observed when the heterocyclic ring was 2,6-disubstituted with bulky groups such as nPr, iPr and especially n-Bu. The same reduced potency was observed for the 3,5-nonane-1,9-diyl derivative **19u**.

The inhibition potency of the representatives **19** with pyridinium ring substituted with groups of low steric demand was quite uniform, all representatives displaying low nanomolar potency against both CA IX and CA XII and validating the proposed design. The similar inhibition profile of sulfonamides **19** against these CA isozymes can be explained considering the structural similarities between the amino acid residues flanking the region of the active site where pyridinium group of these compounds is binding (Figure 2). The general potency of pyridinium derivatives **19** remained relatively high against CA I and especially against CA II due to the structural homology of the active site of these isozymes with CA IX and CA XII. The key residue that probably dictates the isozyme selectivity with these compounds is the residue 131, which is a Val in CA IX, an Ala

in CA XII, a Phe in CA II and a Leu in CA I, since residue 92 is a Gln in all four isozymes. Thus, the space available for pyridinium ring either in the hydrophobic pocket P1 or P2 decreases in the sequence CA XII > CA IX > CA II > CA I. The isozyme selectivity of compounds **19** was found to be highly dependent on the pyridinium ring substitution, as expected. The increase of steric bulk of the substituents (e.g. **19a** → **19e**, **19j** → **19n**, **19o** → **19s**) decreased the potency of the CAI due to the limited size of the hydrophobic pockets P1/P2. The bulkiest representatives **19e**, **19u** and **19s** within these homologous series, as well as other bulky congeners such as **19u**, were most potent against CA XII, followed by CA IX, CA II and CA I, basically mirroring the decrease in P2 pocket volume of these CA isozymes. A nanomolar pan-inhibitor of all four isozymes proved to be **19o** bearing a mixture of small alkyl (methyl) and phenyl substituents on the pyridinium ring. Increase in steric bulk of alkyl substituent within the homologous series (Me → nBu, **19o** → **19s**) diminished significantly the potency of CAIs against CA I, increasing the selectivity of the compounds against this isozyme. The most selective representative was the 2,6-diethyl-4-methylpyridinium benzenesulfonamide **19b**, with selectivity factors of ~ 2 against CA II and ~ 20 against CA I and an excellent potency against CA IX and CA XII. However, it must be emphasized that the selectivity limitations of many of these compounds between CA IX/CA XII and CA I/CA II can be easily overcome considering that both CA IX and CA XII are membrane-bound isozymes, while CA I and CA II are cytosolic enzymes and that the pyridinium benzenesulfonamides **19** are membrane-impermeant due to their salt nature, thus remaining at the exterior of the cell where they can act selectively on the tumor-overexpressed CA IX and CA XII.

Table 1. Inhibition of tumor-associated hCA IX and hCA XII and off-target cytosolic hCA I and hCA II, with pyridinium benzenesulfonamides **19**, and with clinically used CA inhibitor acetazolamide **1**, using the CO₂ hydration assay.

No.	R1	R2	R3	R4	R5	K _I (nM)			
						hCA I	hCA II	hCA IX	hCA XII
1	acetazolamide					250	12	25	5.7
19a	Me	H	Me	H	Me	82.1	1.0	3.2	0.9
19b	Et	H	Me	H	Et	86.3	8.5	4.2	4.0
19c	nPr	H	Me	H	nPr	84.5	7.8	4.5	3.6
19d	iPr	H	Me	H	iPr	33.8	9.6	6.1	5.5
19e	nBu	H	Me	H	nBu	462	58.1	60.4	51.5
19f	Et	H	Me	H	Me	63.6	12.9	6.3	3.7
19g	nPr	H	Me	H	Me	70.1	7.2	6.8	5.4
19h	iPr	H	Me	H	Me	60.7	10.4	6.5	7.4
19i	nBu	H	Me	H	Me	65.1	6.8	5.3	4.0
19j	Me	H	Ph	H	Me	65.3	1.2	2.0	0.87
19k	Et	H	Ph	H	Et	71.6	10.2	9.7	12.1
19l	nPr	H	Ph	H	nPr	75.8	18.0	13.8	21.5
19m	iPr	H	Ph	H	iPr	41.8	9.3	6.4	5.8
19n	nBu	H	Ph	H	nBu	433	49.3	47.1	40.2
19o	Me	H	Ph	H	Ph	8.5	3.4	1.2	0.96
19p	Et	H	Ph	H	Ph	18.0	4.0	3.1	1.4
19q	nPr	H	Ph	H	Ph	24.2	7.8	3.5	2.9
19r	iPr	H	Ph	H	Ph	18.5	8.7	2.9	2.0
19s	nBu	H	Ph	H	Ph	137	43.9	30.8	35.2
19t	Me	Me	Me	H	Me	54.9	2.6	4.3	3.4
19u	Me	3,5-(nonane-1,9-diyl)			Me	256	39.8	33.0	25.1
19v	Me	H	Me	H	Ph	72.3	8.8	5.5	4.7
19w	Ph	H	Me	H	Ph	19.7	6.7	6.6	8.8
19x	Ph	H	Ph	H	Ph	58.0	13.0	14.5	21.7

Molecular Docking

A molecular docking study was performed to investigate the interaction of the four CA isozymes included in this study with selected representative compounds: **19a** with two small substituents in the positions 2 and 6 of the pyridinium ring (dimethyl), **19i** with one small and one long linear substituents (methyl and n-butyl, respectively), and **19e** with two long linear substituents (di-n-butyl) in these positions. The results are presented in Figure 3, showing that the compounds **19a** and **19i** interact with the P1 pocket of hCA I, hCA IX and hCA XII, whereas in hCA II they are positioned in an alternative subpocket pointing towards the His64 residue. This alternative conformation is determined by the bulky Phe131 residue in hCA II, compared with Leu131, Val262 and Ala129 in this position for hCA I, hCA IX and hCA XII, respectively. In agreement with the higher K_I values (Table 1), **19e** binds in significantly different conformation compared with **19a** and **19i**, presumably with lower affinity, in order to avoid the steric clashes with the two n-butyl substituents in the positions 2 and 6 of the pyridinium ring (Figure 3). A direct comparison of binding conformations of **19a** compared with those of **19i** and **19e** is shown in Figure S1. The protocol used here was validated by docking compound **15** with the hCA II structure 1ze8 [58], with a root-mean-square deviation (RMSD) between the docking and X-ray conformations of **15**, calculated for the heavy atoms, of 0.621 Å (Figure S2). The docking study confirms the importance of pyridinium substitution in generating both potency and selectivity between CA isozymes, thus validating the working hypothesis.

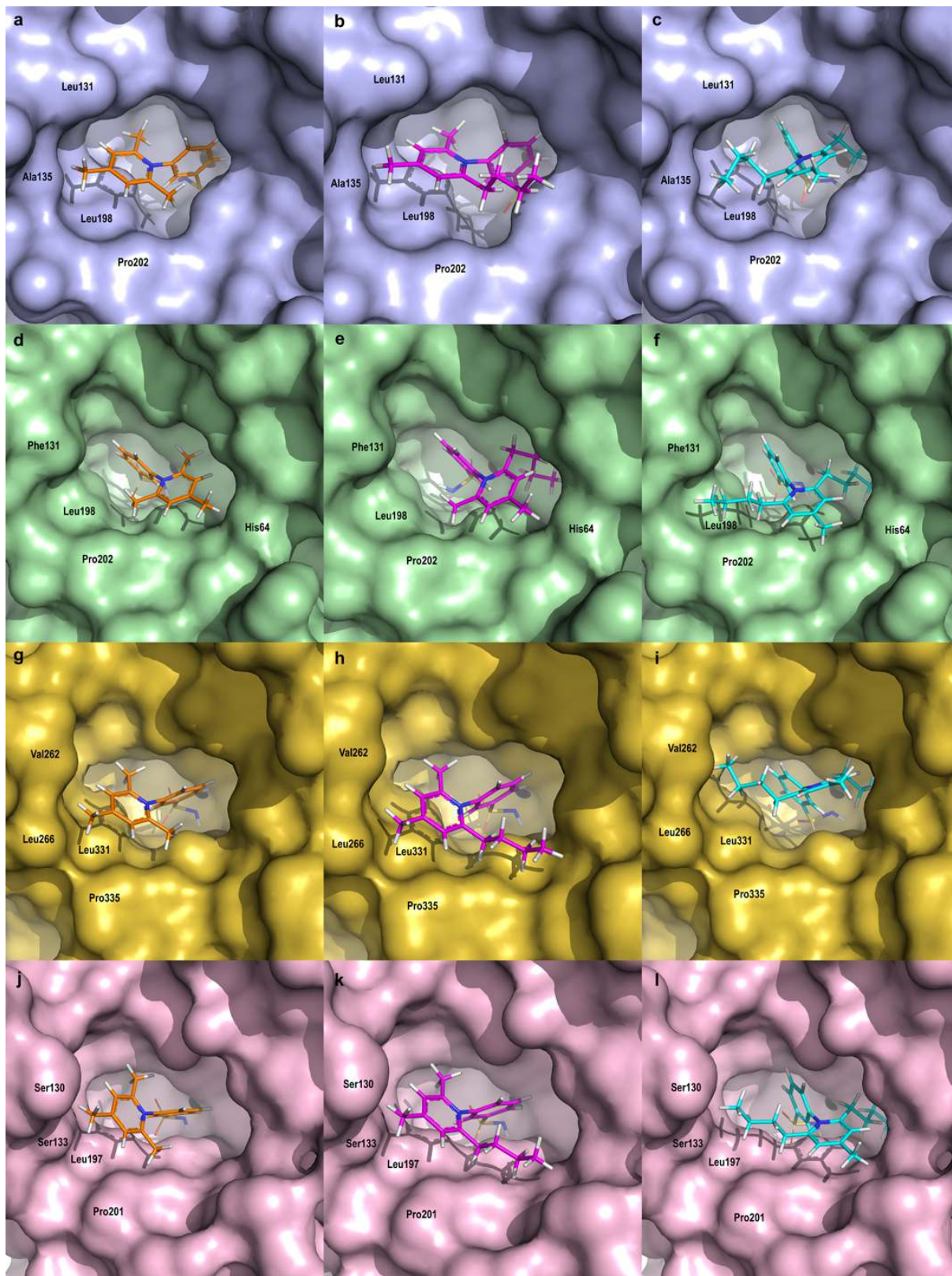


Figure 3. Protein-ligand complexes of selected compounds (**19a**, **19e** and **19i**) with hCA I, hCA II, hCA IX and hCA XII obtained by molecular docking. Proteins are represented as surfaces colored in mauve (hCA I), green (hCA II), yellow (hCA IX) and pink (hCA XII), whereas ligands are represented as sticks colored in orange (**19a**), cyan (**19e**) and magenta (**19i**). Zinc ion is represented as a black sphere.

Cytotoxicity of novel CAIs in normoxic and hypoxic conditions

The cytotoxicity of the most potent pyridinium CAIs was assessed on colon (HT-29), ovarian (SKOV3) and breast (MDA-MB-231) carcinomas. These three cancer cell lines are known to express CA IX and CA XII isozymes, and to over-express these isozymes under hypoxic conditions, thus constituting a robust cellular model for studying the impact of the inhibitors of these isozymes on viability of different tumors [31, 45, 84]. The cancer cells were plated sub-confluent in 96 well plates in normal conditions (37 °C, 5% CO₂ in air, see experimental section). After 24h, when cells were attached, half of the plates from each cell line were incubated in normal (normoxic) conditions and the other half subjected to hypoxia using a hypoxia chamber filled with 1% O₂, 5% CO₂ and 94% N₂ gas mixture to induce the expression of tumoral CA isozymes. After another 24 h of normoxia/hypoxia, cells were treated with CAIs solutions in media at two different concentrations (1 mM, 100 μM) and incubated under normoxic/hypoxic conditions for another 48h. We have selected for testing CAIs **19a** (potent against CA II, CA IX, CA XII), **19f**, **19g**, **19h**, **19i** (superior homologs of **19a** with increased lipophilicity, having similar (nanomolar) CA IX and CA XII potency) and **19e**, **19n** (weakest CAIs in all series, with high lipophilicity). Viability of cells was measured using a standard MTT assay [45] against a control that received only media

with 10% FBS. Acetazolamide **1** was used as positive control, at the same concentrations (Figure 4).

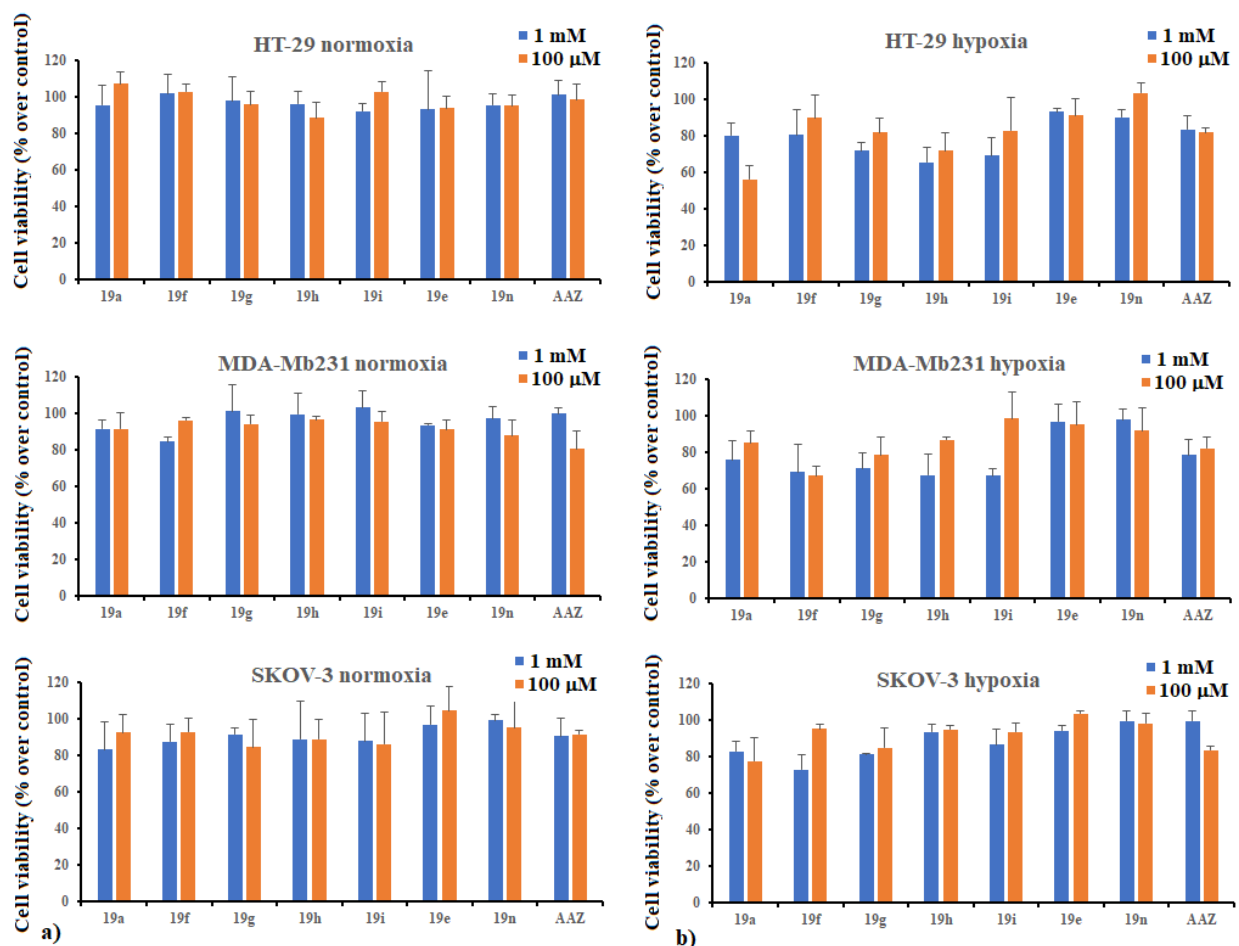


Figure 4. Effect of selected pyridinium sulfonamide CAIs **19** and of acetazolamide **1** (as positive control) at different concentrations (1 mM, 100 μM) on the viability of colon HT-29, breast MDA-MB231 and ovarian SKOV-3 cancer cell lines under normoxic (a) and hypoxic (b) conditions.

Data from Figure 4 reveals that under normoxic conditions CAIs **19** had a limited impact on the growth of the three types of human carcinomas, at both concentrations of 1 mM and 100 μM, similar to acetazolamide **1**. The most susceptible to inhibition with these compounds proved to be the ovarian cancer cell line SKOV-3, for which an 20% decrease of cell viability was observed

with CAI **19a** at the highest concentration of 1 mM. Pyridinium sulfonamides **19a** and its superior homolog **19f** were among the most efficient inhibitors for the growth of colon cancer HT-29 and breast cancer MDA-MB231 under normoxic conditions. However, their effect increased dramatically under hypoxic conditions, when CA IX and CA XII are over-expressed. Growth inhibition of about 30-40 % (corresponding to cell viabilities of 60-70%) were observed with **19a** and **19f**, against all three cancer cell lines, in good agreement with their CA IX and CA XII potency. The decrease in viability achieved with these inhibitors was 10-20% stronger than the effect of acetazolamide **1**, especially at the high concentration of 1 mM. Superior homologs **19g**, **19h** and **19i** had a less pronounced impact than **19a** and **19f**, in agreement with their slightly reduced CA IX and Ca XII potency. The linear increase in lipophilicity of the CAIs **19** did not translated into significant biological effects, indicating that CA IX and CA XII potency remain the most impactful parameter for growth inhibition. Weak inhibitors such as **19e** and **19n** failed to decrease the viability of the three carcinomas, as expected. The effect of the inhibitors was cell type dependent, similarly to the normoxic conditions (Figure 4).

Conclusions

We successfully designed, synthesized, purified a series of pyridinium sulfonamides **19** derived from 3-aminobenzenesulfonamide that allowed efficient sampling of the hydrophobic pockets of the active site of CA. We assessed the inhibition potency of these compounds against tumor over-expressed membrane bound CA isozymes hCA IX and hCA XII, as well as against two off-target CA isozymes – the cytosolic hCA I and hCA II. We identified nanomolar-potent inhibitors against hCA IX and hCA XII, some displaying moderate selectivity for the two off-

target isozymes hCA I and hCA II, thus validating our proposed designs and the working hypothesis of this study. Docking studies performed on selected inhibitors indicated a preference of these new pyridinium sulfonamides for the P1 pocket of the CAs. The charged nature of these inhibitors makes them membrane-impermeant, thus maximizing the selectivity of these compounds for tumor over-expressed isozymes. This was reflected in the positive biological effects observed with selected inhibitors on the growth inhibition of three different carcinomas expressing CA IX and CA XII, especially under hypoxic conditions where these isozymes are over-expressed.

Acknowledgements

MAI acknowledges the financial support of NIH (Grant R03EB026189) and of Edward N. & Della Thome Memorial Foundation. Suleyman Akocak acknowledges the financial support of the Turkish Minister of Education for a PhD scholarship. Ö.G.A. is grateful to TUBITAK (Ankara, Turkey) for the providing financing under the contract no. 2219/2008. This work was also funded by the Italian Ministry for University and Research (MIUR), grant PRIN: rot. 2017XYBP2R (to CTS).

References

1. Hanahan, D. and Robert A. Weinberg, *Hallmarks of Cancer: The Next Generation*. Cell, 2011. **144**(5): p. 646-674.
2. Harris, A.L., *Hypoxia--a key regulatory factor in tumour growth*. Nature reviews. Cancer, 2002. **2**(1): p. 38-47.
3. Yu, A.Y., M.G. Frid, L.A. Shimoda, C.M. Wiener, K. Stenmark, and G.L. Semenza, *Temporal, spatial, and oxygen-regulated expression of hypoxia-inducible factor-1 in the lung*. Am J Physiol, 1998. **275**(4 Pt 1): p. L818-26.
4. Semenza, G.L., *Hydroxylation of HIF-1: oxygen sensing at the molecular level*. Physiology (Bethesda), 2004. **19**: p. 176-82.
5. Semenza, G.L., *Hypoxia-inducible factors: mediators of cancer progression and targets for cancer therapy*. Trends Pharmacol Sci, 2012. **33**(4): p. 207-14.
6. Wouters, A., B. Pauwels, F. Lardon, and J.B. Vermorken, *Review: implications of in vitro research on the effect of radiotherapy and chemotherapy under hypoxic conditions*. Oncologist, 2007. **12**(6): p. 690-712.
7. Supuran, C.T., *Carbonic anhydrases: novel therapeutic applications for inhibitors and activators*. Nature Reviews Drug Discovery, 2008. **7**: p. 168-181.
8. Pastorek, J., S. Pastorekova, I. Callebaut, J.P. Mornon, V. Zelnik, R. Opavsky, M. Zat'ovicova, S. Liao, D. Portetelle, E.J. Stanbridge, and et al., *Cloning and characterization of MN, a human tumor-associated protein with a domain homologous to carbonic anhydrase and a putative helix-loop-helix DNA binding segment*. Oncogene, 1994. **9**(10): p. 2877-88.
9. Pastorekova, S. and J. Pastorek, *Cancer-related carbonic anhydrase isozymes and their inhibition*. Carbonic Anhydrase, 2004: p. 255-281.
10. Alterio, V., M. Hilvo, A. Di Fiore, C.T. Supuran, P. Pan, S. Parkkila, A. Scaloni, J. Pastorek, S. Pastorekova, C. Pedone, A. Scozzafava, S.M. Monti, and G. De Simone, *Crystal structure of the catalytic domain of the tumor-associated human carbonic anhydrase IX*. Proc Natl Acad Sci U S A, 2009. **106**(38): p. 16233-8.
11. Wykoff, C.C., N.J. Beasley, P.H. Watson, K.J. Turner, J. Pastorek, A. Sibtain, G.D. Wilson, H. Turley, K.L. Talks, P.H. Maxwell, C.W. Pugh, P.J. Ratcliffe, and A.L. Harris, *Hypoxia-inducible expression of tumor-associated carbonic anhydrases*. Cancer Res, 2000. **60**(24): p. 7075-83.
12. Potter, C. and A.L. Harris, *Hypoxia inducible carbonic anhydrase IX, marker of tumour hypoxia, survival pathway and therapy target*. Cell Cycle, 2004. **3**(2): p. 164-7.
13. Hussain, S.A., D.H. Palmer, R. Ganesan, L. Hiller, J. Gregory, P.G. Murray, J. Pastorek, L. Young, and N.D. James, *Carbonic anhydrase IX, a marker of hypoxia: correlation with clinical outcome in transitional cell carcinoma of the bladder*. Oncol Rep, 2004. **11**(5): p. 1005-10.
14. Jarvela, S., S. Parkkila, H. Bragge, M. Kahkonen, A.K. Parkkila, Y. Soini, S. Pastorekova, J. Pastorek, and H. Haapasalo, *Carbonic anhydrase IX in oligodendroglial brain tumors*. BMC Cancer, 2008. **8**: p. 1.
15. Kivela, A.J., S. Parkkila, J. Saarnio, T.J. Karttunen, J. Kivela, A.K. Parkkila, S. Pastorekova, J. Pastorek, A. Waheed, W.S. Sly, and H. Rajaniemi, *Expression of transmembrane carbonic anhydrase isoenzymes IX and XII in normal human pancreas and pancreatic tumours*. Histochem Cell Biol, 2000. **114**(3): p. 197-204.
16. Hussain, S.A., R. Ganesan, G. Reynolds, L. Gross, A. Stevens, J. Pastorek, P.G. Murray, B. Perunovic, M.S. Anwar, L. Billingham, N.D. James, D. Spooner, C.J. Poole, D.W. Rea, and D.H. Palmer, *Hypoxia-regulated carbonic anhydrase IX expression is associated with poor survival in patients with invasive breast cancer*. Br J Cancer, 2007. **96**(1): p. 104-9.
17. Pastorek, J. and S. Pastorekova, *Hypoxia-induced carbonic anhydrase IX as a target for cancer therapy: from biology to clinical use*. Semin Cancer Biol, 2015. **31**: p. 52-64.
18. Guler, O.O., G. De Simone, and C.T. Supuran, *Drug design studies of the novel antitumor targets carbonic anhydrase IX and XII*. Curr Med Chem, 2010. **17**(15): p. 1516-26.

19. Scheurer, S.B., J.N. Rybak, C. Rosli, D. Neri, and G. Elia, *Modulation of gene expression by hypoxia in human umbilical cord vein endothelial cells: A transcriptomic and proteomic study*. Proteomics, 2004. **4**(6): p. 1737-60.
20. Neri, D. and C.T. Supuran, *Interfering with pH regulation in tumours as a therapeutic strategy*. Nat Rev Drug Discov, 2011. **10**(10): p. 767-77.
21. Pastorekova, S., S. Parkkila, A.K. Parkkila, R. Opavsky, V. Zelnik, J. Saarnio, and J. Pastorek, *Carbonic anhydrase IX, MN/CA IX: analysis of stomach complementary DNA sequence and expression in human and rat alimentary tracts*. Gastroenterology, 1997. **112**(2): p. 398-408.
22. Tureci, O., U. Sahin, E. Vollmar, S. Siemer, E. Gottert, G. Seitz, A.K. Parkkila, G.N. Shah, J.H. Grubb, M. Pfreundschuh, and W.S. Sly, *Human carbonic anhydrase XII: cDNA cloning, expression, and chromosomal localization of a carbonic anhydrase gene that is overexpressed in some renal cell cancers*. Proc Natl Acad Sci U S A, 1998. **95**(13): p. 7608-13.
23. Whittington, D.A., A. Waheed, B. Ulmasov, G.N. Shah, J.H. Grubb, W.S. Sly, and D.W. Christianson, *Crystal structure of the dimeric extracellular domain of human carbonic anhydrase XII, a bitopic membrane protein overexpressed in certain cancer tumor cells*. Proc Natl Acad Sci U S A, 2001. **98**(17): p. 9545-50.
24. Ulmasov, B., A. Waheed, G.N. Shah, J.H. Grubb, W.S. Sly, C. Tu, and D.N. Silverman, *Purification and kinetic analysis of recombinant CA XII, a membrane carbonic anhydrase overexpressed in certain cancers*. Proc Natl Acad Sci U S A, 2000. **97**(26): p. 14212-7.
25. Zamanova, S., A.M. Shabana, U.K. Mondal, and M.A. Ilies, *Carbonic anhydrases as disease markers*. Expert Opin Ther Pat, 2019. **29**(7): p. 509-533.
26. Robertson, N., C. Potter, and A.L. Harris, *Role of carbonic anhydrase IX in human tumor cell growth, survival, and invasion*. Cancer Res, 2004. **64**(17): p. 6160-5.
27. Swietach, P., S. Wigfield, P. Cobden, C.T. Supuran, A.L. Harris, and R.D. Vaughan-Jones, *Tumor-associated carbonic anhydrase 9 spatially coordinates intracellular pH in three-dimensional multicellular growths*. J Biol Chem, 2008. **283**(29): p. 20473-83.
28. Chiche, J., K. Ilc, J. Laferriere, E. Trottier, F. Dayan, N.M. Mazure, M.C. Brahimi-Horn, and J. Pouyssegur, *Hypoxia-inducible carbonic anhydrase IX and XII promote tumor cell growth by counteracting acidosis through the regulation of the intracellular pH*. Cancer Res, 2009. **69**(1): p. 358-68.
29. Parks, S.K., J. Chiche, and J. Pouyssegur, *pH control mechanisms of tumor survival and growth*. J Cell Physiol, 2011. **226**(2): p. 299-308.
30. Supuran, C.T., *Carbonic anhydrase inhibitors as emerging agents for the treatment and imaging of hypoxic tumors*. Expert Opin Investig Drugs, 2018. **27**(12): p. 963-970.
31. Shabana, A.M. and M.A. Ilies, *Drug Delivery to Hypoxic Tumors Targeting Carbonic Anhydrase IX*, in *Targeted Nanosystems for Therapeutic Applications: New Concepts, Dynamic Properties, Efficiency, and Toxicity*. 2019, American Chemical Society. p. 223-252.
32. Alterio, V., A. Di Fiore, K. D'Ambrosio, C.T. Supuran, and G. De Simone, *Multiple binding modes of inhibitors to carbonic anhydrases: how to design specific drugs targeting 15 different isoforms?* Chem Rev, 2012. **112**(8): p. 4421-68.
33. Supuran, C.T., *Structure and function of carbonic anhydrases*. Biochem J, 2016. **473**(14): p. 2023-32.
34. Supuran, C.T., *A Simple Yet Multifaceted Enzyme*. Rev Chim, 2020. **71**(5): p. 1-16.
35. Akocak, S. and C.T. Supuran, *Activation of α -, β -, γ - δ -, ζ - and η - class of carbonic anhydrases with amines and amino acids: a review*. J Enzyme Inhib Med Chem, 2019. **34**(1): p. 1652-1659.
36. Lolak, N., S. Akocak, S. Bua, and C.T. Supuran, *Design, synthesis and biological evaluation of novel ureido benzenesulfonamides incorporating 1,3,5-triazine moieties as potent carbonic anhydrase IX inhibitors*. Bioorg Chem, 2019. **82**: p. 117-122.
37. Parkkila, S., H. Rajaniemi, A.K. Parkkila, J. Kivela, A. Waheed, S. Pastorekova, J. Pastorek, and W.S. Sly, *Carbonic anhydrase inhibitor suppresses invasion of renal cancer cells in vitro*. Proc Natl Acad Sci U S A, 2000. **97**(5): p. 2220-4.

38. Krishnamurthy, V.M., G.K. Kaufman, A.R. Urbach, I. Gitlin, K.L. Gudiksen, D.B. Weibel, and G.M. Whitesides, *Carbonic anhydrase as a model for biophysical and physical-organic studies of proteins and protein-ligand binding*. Chem Rev, 2008. **108**(3): p. 946-1051.
39. McDonald, P.C., J.Y. Winum, C.T. Supuran, and S. Dedhar, *Recent developments in targeting carbonic anhydrase IX for cancer therapeutics*. Oncotarget, 2012. **3**(1): p. 84-97.
40. Ilies, M.A., D. Vullo, J. Pastorek, A. Scozzafava, M. Ilies, M.T. Caproiu, S. Pastorekova, and C.T. Supuran, *Carbonic anhydrase inhibitors. Inhibition of tumor-associated isozyme IX by halogenosulfanilamide and halogenophenylaminobenzolamide derivatives*. J Med Chem, 2003. **46**(11): p. 2187-96.
41. McKenna, R. and C.T. Supuran, *Carbonic anhydrase inhibitors drug design*. Subcell Biochem, 2014. **75**: p. 291-323.
42. Akocak, S. and M.A. Ilies, *Next generation primary sulfonamide carbonic anhydrase inhibitors*, in *Targeting carbonic anhydrases*, C.T. Supuran and C. Capasso, Editors. 2014, Future Science: London. p. 3-19.
43. Supuran, C.T. and J.Y. Winum, *Carbonic anhydrase IX inhibitors in cancer therapy: an update*. Future Med Chem, 2015. **7**(11): p. 1407-14.
44. Supuran, C.T. and J.Y. Winum, *Designing carbonic anhydrase inhibitors for the treatment of breast cancer*. Expert Opin Drug Discov, 2015. **10**(6): p. 591-7.
45. Akocak, S., M.R. Alam, A.M. Shabana, R.K.K. Sanku, D. Vullo, H. Thompson, E.R. Swenson, C.T. Supuran, and M.A. Ilies, *PEGylated Bis-Sulfonamide Carbonic Anhydrase Inhibitors Can Efficiently Control the Growth of Several Carbonic Anhydrase IX-Expressing Carcinomas*. Journal of Medicinal Chemistry, 2016. **59**(10): p. 5077-5088.
46. Nocentini, A. and C.T. Supuran, *Carbonic anhydrase inhibitors as antitumor/antimetastatic agents: a patent review (2008-2018)*. Expert Opin Ther Pat, 2018. **28**(10): p. 729-740.
47. Shabana, A.M., U.K. Mondal, M.R. Alam, T. Spoon, C.A. Ross, M. Madesh, C.T. Supuran, and M.A. Ilies, *pH-Sensitive Multiligand Gold Nanoplatfom Targeting Carbonic Anhydrase IX Enhances the Delivery of Doxorubicin to Hypoxic Tumor Spheroids and Overcomes the Hypoxia-Induced Chemoresistance*. ACS Appl Mater Interfaces, 2018. **10**(21): p. 17792-17808.
48. Bozdog, M., A.S.A. Altamimi, D. Vullo, C.T. Supuran, and F. Carta, *State of the Art on Carbonic Anhydrase Modulators for Biomedical Purposes*. Curr Med Chem, 2019. **26**(15): p. 2558-2573.
49. Ilies, M.A. and J.-Y. Winum, *Chapter 16 - Carbonic anhydrase inhibitors for the treatment of tumors: therapeutic, immunologic, and diagnostic tools targeting isoforms IX and XII*, in *Carbonic Anhydrases*, C.T. Supuran and A. Nocentini, Editors. 2019, Academic Press. p. 331-365.
50. Akocak, S., N. Lolak, A. Nocentini, G. Karakoc, A. Tufan, and C.T. Supuran, *Synthesis and biological evaluation of novel aromatic and heterocyclic bis-sulfonamide Schiff bases as carbonic anhydrase I, II, VII and IX inhibitors*. Bioorg Med Chem, 2017. **25**(12): p. 3093-3097.
51. Scozzafava, A. and C.T. Supuran, *Glaucoma and the applications of carbonic anhydrase inhibitors*. Subcell Biochem, 2014. **75**: p. 349-59.
52. Lolak, N., S. Akocak, S. Bua, R.K.K. Sanku, and C.T. Supuran, *Discovery of new ureido benzenesulfonamides incorporating 1,3,5-triazine moieties as carbonic anhydrase I, II, IX and XII inhibitors*. Bioorg Med Chem, 2019. **27**(8): p. 1588-1594.
53. Ilies, M.A., B. Masereel, S. Rolin, A. Scozzafava, G. Campeanu, V. Cimpeanu, and C.T. Supuran, *Carbonic anhydrase inhibitors: aromatic and heterocyclic sulfonamides incorporating adamantyl moieties with strong anticonvulsant activity*. Bioorg Med Chem, 2004. **12**(10): p. 2717-26.
54. Avvaru, B.S., J.M. Wagner, A. Maresca, A. Scozzafava, A.H. Robbins, C.T. Supuran, and R. McKenna, *Carbonic anhydrase inhibitors. The X-ray crystal structure of human isoform II in adduct with an adamantyl analogue of acetazolamide resides in a less utilized binding pocket than most hydrophobic inhibitors*. Bioorg Med Chem Lett, 2010. **20**(15): p. 4376-81.

55. Casini, A., F. Mincione, M.A. Ilies, L. Menabuoni, A. Scozzafava, and C.T. Supuran, *Carbonic anhydrase inhibitors: synthesis and inhibition against isozymes I, II and IV of topically acting antiglaucoma sulfonamides incorporating cis-5-norbornene-endo-3-carboxy-2-carboxamido moieties*. J Enzyme Inhib, 2001. **16**(2): p. 113-23.
56. Menchise, V., G. De Simone, A. Di Fiore, A. Scozzafava, and C.T. Supuran, *Carbonic anhydrase inhibitors: X-ray crystallographic studies for the binding of 5-amino-1,3,4-thiadiazole-2-sulfonamide and 5-(4-amino-3-chloro-5-fluorophenylsulfonamido)-1,3,4-thiadiazole-2-sulfonamide to human isoform II*. Bioorg Med Chem Lett, 2006. **16**(24): p. 6204-8.
57. Biswas, S., F. Carta, A. Scozzafava, R. McKenna, and C.T. Supuran, *Structural effect of phenyl ring compared to thiadiazole based adamantyl-sulfonamides on carbonic anhydrase inhibition*. Bioorganic & medicinal chemistry, 2013. **21**(8): p. 2314-8.
58. Menchise, V., G. De Simone, V. Alterio, A. Di Fiore, C. Pedone, A. Scozzafava, and C.T. Supuran, *Carbonic anhydrase inhibitors: stacking with Phe131 determines active site binding region of inhibitors as exemplified by the X-ray crystal structure of a membrane-impermeant antitumor sulfonamide complexed with isozyme II*. J Med Chem, 2005. **48**(18): p. 5721-7.
59. Tinker, J.P., R. Coulson, and I.M. Weiner, *Dextran-bound inhibitors of carbonic anhydrase*. J Pharmacol Exp Ther, 1981. **218**(3): p. 600-7.
60. Maren, T.H., C.W. Conroy, G.C. Wynns, and D.R. Godman, *Renal and cerebrospinal fluid formation pharmacology of a high molecular weight carbonic anhydrase inhibitor*. J Pharmacol Exp Ther, 1997. **280**(1): p. 98-104.
61. Winum, J.Y., A. Casini, F. Mincione, M. Starnotti, J.L. Montero, A. Scozzafava, and C.T. Supuran, *Carbonic anhydrase inhibitors: N-(p-sulfamoylphenyl)-alpha-D-glycopyranosylamines as topically acting antiglaucoma agents in hypertensive rabbits*. Bioorg Med Chem Lett, 2004. **14**(1): p. 225-9.
62. Wilkinson, B.L., L.F. Bornaghi, T.A. Houston, A. Innocenti, C.T. Supuran, and S.A. Poulsen, *A novel class of carbonic anhydrase inhibitors: glycoconjugate benzene sulfonamides prepared by "click-tailing"*. J Med Chem, 2006. **49**(22): p. 6539-48.
63. Smaine, F.Z., J.Y. Winum, J.L. Montero, Z. Regainia, D. Vullo, A. Scozzafava, and C.T. Supuran, *Carbonic anhydrase inhibitors: Selective inhibition of the extracellular, tumor-associated isoforms IX and XII over isozymes I and II with glycosyl-thioureido-sulfonamides*. Bioorg Med Chem Lett, 2007. **17**(18): p. 5096-100.
64. Lopez, M., L.F. Bornaghi, A. Innocenti, D. Vullo, S.A. Charman, C.T. Supuran, and S.A. Poulsen, *Sulfonamide linked neoglycoconjugates--a new class of inhibitors for cancer-associated carbonic anhydrases*. Journal of medicinal chemistry, 2010. **53**(7): p. 2913-26.
65. Morris, J.C., J. Chiche, C. Grellier, M. Lopez, L.F. Bornaghi, A. Maresca, C.T. Supuran, J. Pouyssegur, and S.A. Poulsen, *Targeting hypoxic tumor cell viability with carbohydrate-based carbonic anhydrase IX and XII inhibitors*. Journal of medicinal chemistry, 2011. **54**(19): p. 6905-18.
66. Moeker, J., K. Teruya, S. Rossit, B.L. Wilkinson, M. Lopez, L.F. Bornaghi, A. Innocenti, C.T. Supuran, and S.A. Poulsen, *Design and synthesis of thiourea compounds that inhibit transmembrane anchored carbonic anhydrases*. Bioorganic & medicinal chemistry, 2012. **20**(7): p. 2392-404.
67. Supuran, C.T., G. Manole, A. Dinculescu, A. Schiketanz, M.D. Gheorghiu, I. Puscas, and A.T. Balaban, *Carbonic anhydrase inhibitors. V: Pyrylium salts in the synthesis of isozyme-specific inhibitors*. J Pharm Sci, 1992. **81**(7): p. 716-9.
68. Supuran, C.T., M.A. Ilies, and A. Scozzafava, *Carbonic anhydrase inhibitors - Part 29: Interaction of isozymes I, II and IV with benzolamide-like derivatives*. European Journal of Medicinal Chemistry, 1998. **33**: p. 739-751.
69. Supuran, C.T., A. Scozzafava, M.A. Ilies, B. Iorga, T. Cristea, F. Briganti, F. Chiraleu, and M.D. Banciu, *Carbonic anhydrase inhibitors - Part 53 - Synthesis of substituted-pyridinium derivatives*

- of aromatic sulfonamides: The first non-polymeric membrane-impermeable inhibitors with selectivity for isozyme IV.* European Journal of Medicinal Chemistry, 1998. **33**(7-8): p. 577-594.
70. Scozzafava, A., F. Briganti, M.A. Ilies, and C.T. Supuran, *Carbonic anhydrase inhibitors: synthesis of membrane-impermeant low molecular weight sulfonamides possessing in vivo selectivity for the membrane-bound versus cytosolic isozymes.* J Med Chem, 2000. **43**(2): p. 292-300.
 71. Supuran, C.T., A. Scozzafava, M.A. Ilies, and F. Briganti, *Carbonic anhydrase inhibitors: synthesis of sulfonamides incorporating 2,4,6-trisubstituted-pyridinium-ethylcarboxamido moieties possessing membrane-impermeability and in vivo selectivity for the membrane-bound (CA IV) versus the cytosolic (CA I and CA II) isozymes.* J Enzyme Inhib, 2000. **15**(4): p. 381-401.
 72. Pastorekova, S., A. Casini, A. Scozzafava, D. Vullo, J. Pastorek, and C.T. Supuran, *Carbonic anhydrase inhibitors: the first selective, membrane-impermeant inhibitors targeting the tumor-associated isozyme IX.* Bioorg Med Chem Lett, 2004. **14**(4): p. 869-73.
 73. Casey, J.R., P.E. Morgan, D. Vullo, A. Scozzafava, A. Mastrolorenzo, and C.T. Supuran, *Carbonic anhydrase inhibitors. Design of selective, membrane-impermeant inhibitors targeting the human tumor-associated isozyme IX.* J Med Chem, 2004. **47**(9): p. 2337-47.
 74. Di Cesare Mannelli, L., L. Micheli, F. Carta, A. Cozzi, C. Ghelardini, and C.T. Supuran, *Carbonic anhydrase inhibition for the management of cerebral ischemia: in vivo evaluation of sulfonamide and coumarin inhibitors.* J Enzyme Inhib Med Chem, 2016. **31**(6): p. 894-9.
 75. Bhatt, A., U.K. Mondal, C.T. Supuran, M.A. Ilies, and R. McKenna, *Crystal Structure of Carbonic Anhydrase II in Complex with an Activating Ligand: Implications in Neuronal Function.* Mol Neurobiol, 2018. **55**(9): p. 7431-7437.
 76. Draghici, B., D. Vullo, S. Akocak, E.A. Walker, C.T. Supuran, and M.A. Ilies, *Ethylene bis-imidazoles are highly potent and selective activators for isozymes VA and VII of carbonic anhydrase, with a potential nootropic effect.* Chem Commun (Camb), 2014. **50**(45): p. 5980-3.
 77. Ilies, M., M.D. Banciu, M.A. Ilies, A. Scozzafava, M.T. Caproiu, and C.T. Supuran, *Carbonic Anhydrase Activators: Design of High Affinity Isozymes I, II, and IV Activators, Incorporating Tri-/Tetrasubstituted-pyridinium-azole Moieties.* Journal of Medicinal Chemistry, 2002. **45**(2): p. 504-510.
 78. Balaban, T.S. and A.T. Balaban, *Pyrylium Salts*, in *Science of Synthesis. Houben-Weyl Methods of Molecular Transformations*, T.E. J., Editor. 2003, G. Thieme Verlag: Stuttgart. p. 11-200.
 79. Rami, M., L. Dubois, N.K. Parvathaneni, V. Alterio, S.J. van Kuijk, S.M. Monti, P. Lambin, G. De Simone, C.T. Supuran, and J.Y. Winum, *Hypoxia-Targeting Carbonic Anhydrase IX Inhibitors by a New Series of Nitroimidazole-Sulfonamides/Sulfamides/Sulfamates.* Journal of medicinal chemistry, 2013.
 80. Khalifah, R.G., *The carbon dioxide hydration activity of carbonic anhydrase. I. Stop-flow kinetic studies on the native human isoenzymes B and C.* J Biol Chem, 1971. **246**(8): p. 2561-73.
 81. Verdonk, M.L., J.C. Cole, M.J. Hartshorn, C.W. Murray, and R.D. Taylor, *Improved protein-ligand docking using GOLD.* Proteins, 2003. **52**(4): p. 609-23.
 82. Bozdag, M., F. Carta, M. Ceruso, M. Ferraroni, P.C. McDonald, S. Dedhar, and C.T. Supuran, *Discovery of 4-Hydroxy-3-(3-(phenylureido)benzenesulfonamides as SLC-0111 Analogues for the Treatment of Hypoxic Tumors Overexpressing Carbonic Anhydrase IX.* J Med Chem, 2018. **61**(14): p. 6328-6338.
 83. Koruza, K., B. Lafumat, M. Nyblom, B.P. Mahon, W. Knecht, R. McKenna, and S.Z. Fisher, *Structural comparison of protiated, H/D-exchanged and deuterated human carbonic anhydrase IX.* Acta Crystallogr D Struct Biol, 2019. **75**(Pt 10): p. 895-903.
 84. Kazokaitė, J., R. Niemans, V. Dudutienė, H.M. Becker, J. Leitāns, A. Zubrienė, L. Baranauskienė, G. Gondi, R. Zeidler, J. Matulienė, K. Tārs, A. Yaromina, P. Lambin, L.J. Dubois, and D. Matulis, *Novel fluorinated carbonic anhydrase IX inhibitors reduce hypoxia-induced acidification and clonogenic survival of cancer cells.* Oncotarget; Vol 9, No 42, 2018.

Supplemental Information

Pyridinium Derivatives of 3-Aminobenzenesulfonamide are Nanomolar-potent Inhibitors of Tumor-expressed Carbonic Anhydrase Isozymes CA IX and CA XII

Suleyman Akocak,^a Özlen Güzel-Akdemir,^{b,c} Rajesh Kishore Kumar Sanku,^a Samson S. Russom^a, Bogdan I. Iorga,^d Claudiu T. Supuran,^{b*} and Marc A. Ilies^{a*}

^a Department of Pharmaceutical Sciences and Moulder Center for Drug Discovery Research, Temple University School of Pharmacy, 3307 N Broad Street, Philadelphia, PA-19140.

^b NEUROFARBA Department, Università degli Studi di Firenze, Polo Scientifico, Via della Lastruccia 3, 50019 Sesto Fiorentino (Florence), Italy.

^c Istanbul University, Faculty of Pharmacy, Department of Pharmaceutical Chemistry, 34116 Beyazıt, Istanbul, Turkey.

^d Université Paris-Saclay, CNRS, Institut de Chimie des Substances Naturelles (ICSN), 1 Avenue de la Terrasse, 91198 Gif-sur-Yvette, France.

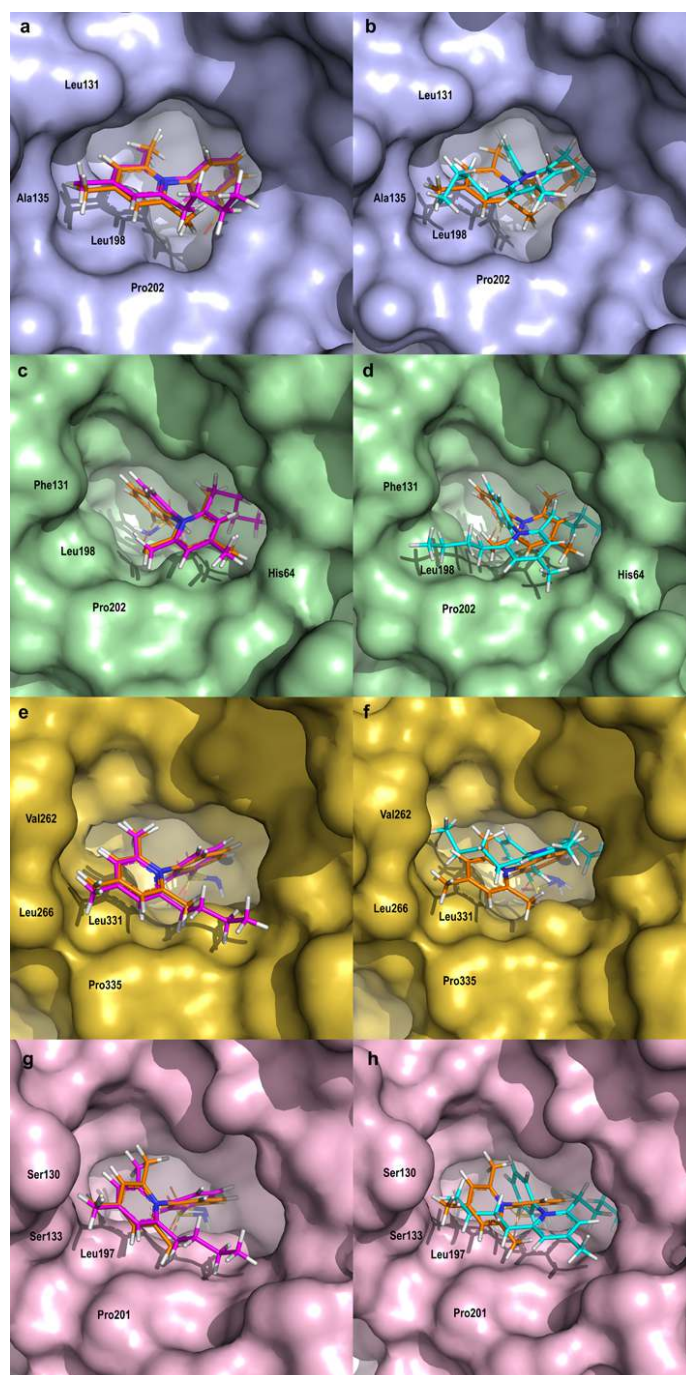


Figure S1. Docking conformations of compounds **19a** and **19i** (**a, c, e, g**) and **19a** and **19e** (**b, d, f, h**) in the active sites of hCA I (**a, b**), hCA II (**c, d**), hCA IX (**e, f**) and hCA XII (**g, h**). Proteins are represented as surfaces colored in mauve (hCA I), green (hCA II), yellow (hCA IX) and pink (hCA XII), whereas ligands are represented as sticks colored in orange (**19a**), cyan (**19e**) and magenta (**19i**). Zinc ion is represented as a black sphere.

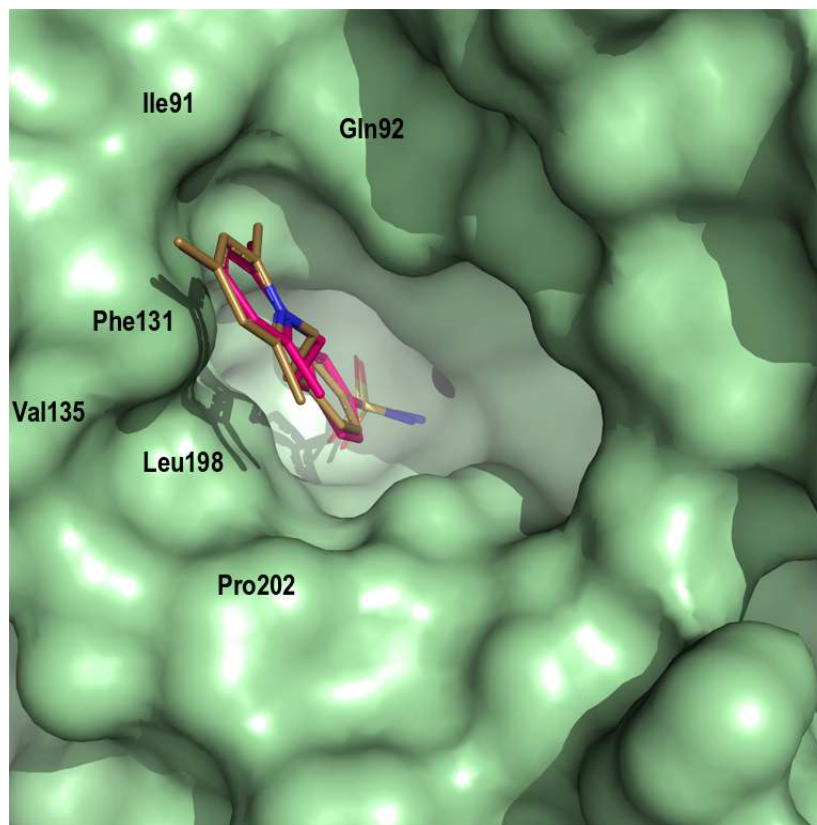
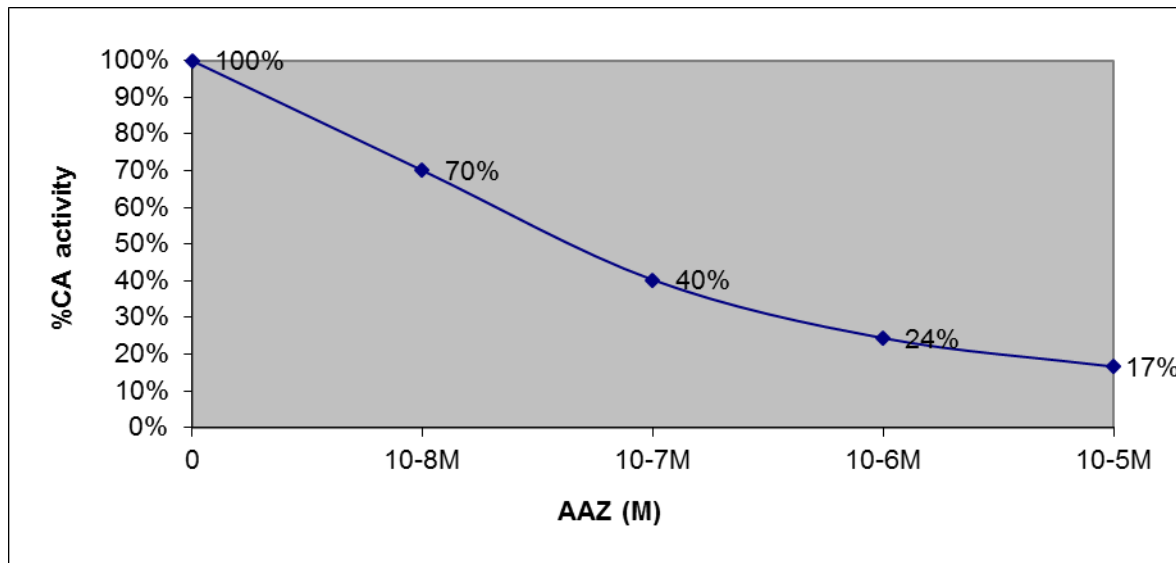
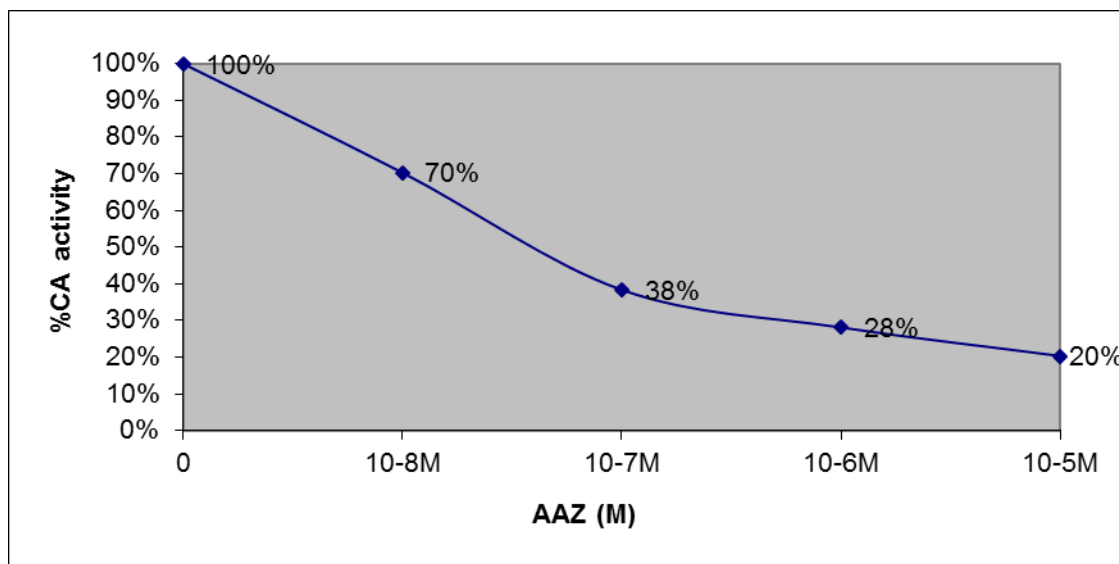


Figure S2. Docking (red carmine) and X-ray (gold, from structure 1ze8 [1]) conformations of compound **15** in the active site of hCA II (represented as surface colored in green). Zinc ion is represented as a black sphere. The root-mean-square deviation (RMSD) between the two conformations (heavy atoms) is 0.621 Å. Hydrogen atoms are omitted for clarity.

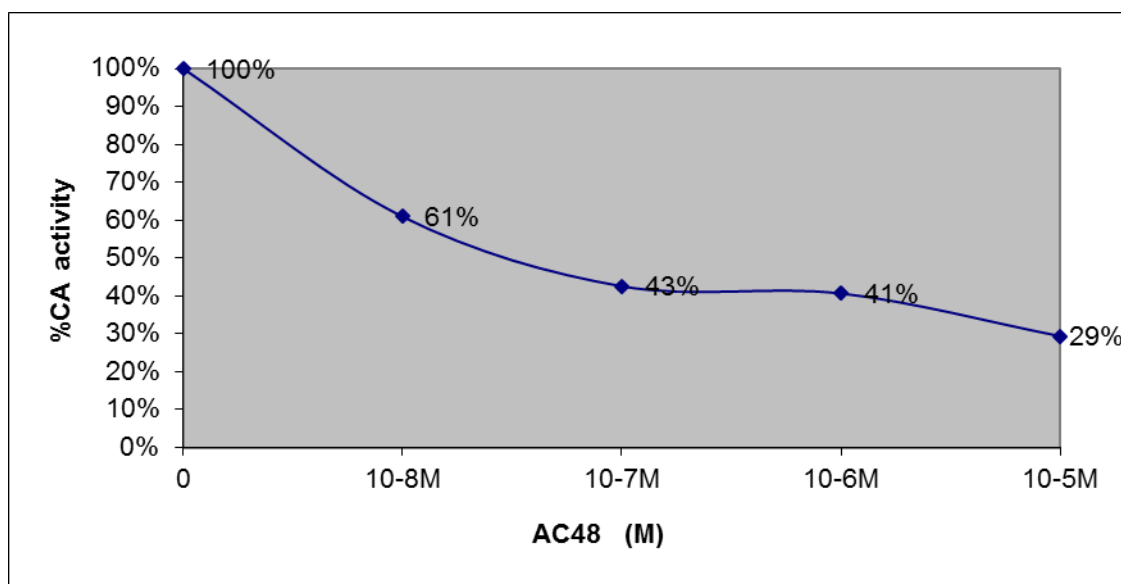
Representative inhibition curves for reported compounds 19 and for the positive control used (acetazolamide 1)



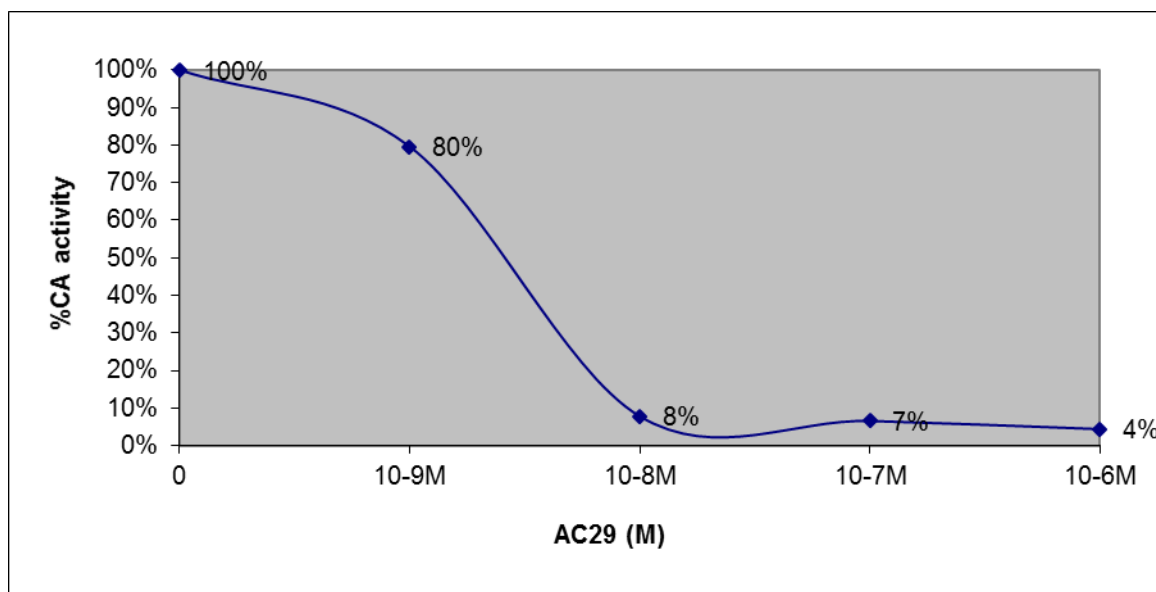
hCA II, with acetazolamide **1**, $K_I = 12$ nM



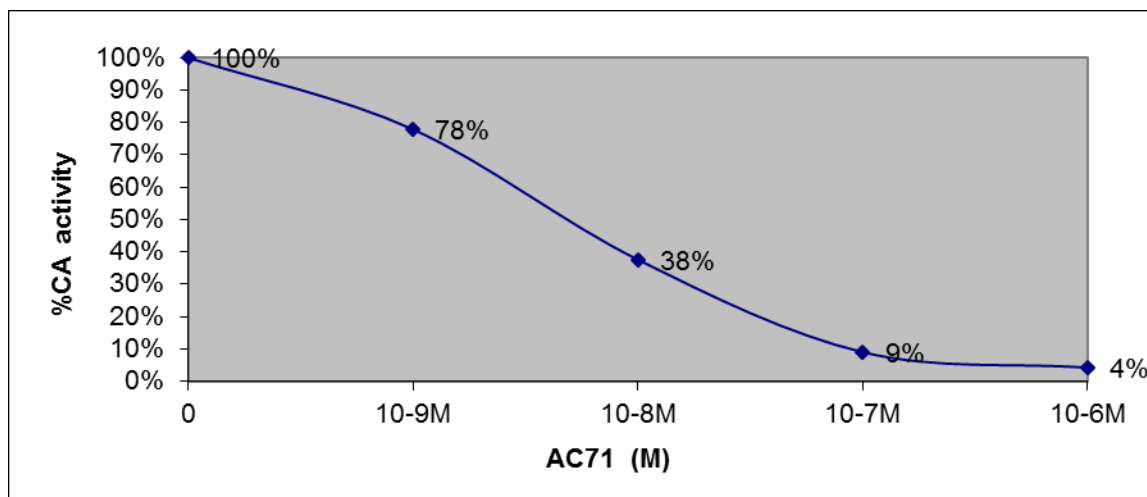
hCA IX, acetazolamide **1**, $K_I = 25$ nM



Compound **19s**, hCA IX, $K_I = 30.8$ nM



Compound **19p**, hCA XII, $K_I = 1.4$ nM



Compound **19w**, hCA XII, $K_I = 8.8$ nM

References

1. Menchise, V., G. De Simone, V. Alterio, A. Di Fiore, C. Pedone, A. Scozzafava, and C.T. Supuran, *Carbonic anhydrase inhibitors: stacking with Phe131 determines active site binding region of inhibitors as exemplified by the X-ray crystal structure of a membrane-impermeant antitumor sulfonamide complexed with isozyme II*. *J Med Chem*, 2005. **48**(18): p. 5721-7.